



Recurring Northward Flow Events in the East Greenland Current: A New Pathway for Atlantic Heat into the Arctic

Rebecca McPherson¹, Wilken-Jon von Appen¹, Laura de Steur², Luise Becker^{1,3}, Monica Ionita¹,
Thomas Krumpfen¹, Gunnar Spreen⁴, Finn Heukamp¹

5 ¹Alfred Wegener Institute, Helmholtz Centre for Polar and Marine Research; Bremerhaven, Germany

²Norwegian Polar Institute; Tromsø, Norway

³Department of Physics, University of Bremen, Bremen, Germany

⁴Institute of Environmental Physics, University of Bremen, Bremen, Germany

Correspondence to: Rebecca McPherson (rebecca.mcpherson@awi.de)

10 **Abstract.** The East Greenland Current (EGC) is the main conveyor of cold, fresh Polar Water and sea
ice from the Arctic Ocean through Fram Strait to the subpolar North Atlantic. Seven years of continuous
mooring observations on the East Greenland continental slope at 79°N (2018–2025) reveal that whilst
the EGC typically maintains a southward flow year-round, it is punctuated by periodic northward flow
15 events on the upper continental slope. The majority are short-lived local events (lasting fewer than 5
days), consistent with mesoscale eddy activity. However, two prolonged deep-reaching events — in
April–May 2019 (29 days) and May–June 2025 (at least 35 days) — were anomalous in their duration,
intensity (i.e. exceeding the climatological mean by 2 - 3 standard deviations), and vertical coherence
(down to at least 500 m depth). During both events, hydrographic observations show anomalous warm
20 Atlantic-origin waters at depths typically occupied by cooler Arctic Atlantic Water, weakened vertical
stratification, and temperature-salinity properties consistent with recent West Spitsbergen Current
recirculation across Fram Strait. An extended mooring record at 78°50'N (2003–2019) identified a
further 7 deep-reaching northward flow events, demonstrating that episodic northward flow is a
recurring intrinsic feature of the EGC system rather than a recent phenomenon. A persistent sea-level
pressure dipole with anomalous northward winds along the East Greenland margin is identified all
25 strong deep northward flow events. It is proposed that this forcing drives a lateral reorganisation of the
boundary current where anomalous eastward Ekman transport displaces the EGC core offshore whilst
geostrophically adjusted flow on the inner slope produces a net northward current inshore. The
anomalously warm AW at depth thus arises through northward advection of recirculating AW and
upwelling over the slope. These anomalous flow events establish an episodic northward pathway for
30 warm Atlantic-origin water with a potential advective reach of perhaps hundreds of kilometres beyond
the mooring location — a previously unidentified pathway of Atlantic heat transport into the Arctic
interior. The co-occurrence of the 2025 event with a record low sea-ice area in July in the northeast
Greenland region suggests that these oceanic events influence regional sea ice variability through
dynamic atmospheric export and ocean-ice interactions, though a direct causal link remains to be
35 established. Whether these events represent rare features of a naturally variable boundary current
system or early signals of ongoing change in the Arctic-Atlantic exchange remains an open question.



1 Introduction

The East Greenland Current (EGC) is the main conveyor of cold, fresh Polar Water (PW) and sea ice from the Arctic Ocean to the subpolar North Atlantic (Aagaard and Coachman, 1968a). From
40 observations spanning northern Fram Strait to Cape Farewell, the EGC has been characterised as a largely continuous southward boundary current pathway along the Greenland margin (Aagaard and Coachman, 1968a, 1968b), linking the Arctic gateway in the north (Håvik et al., 2017) through Denmark Strait and into the subpolar North Atlantic in the south (Le Bras et al., 2018). Flowing southward along the East Greenland continental margin in Fram Strait (Fig. 1), the EGC exports
45 approximately half of the liquid freshwater and nearly 90% of the sea ice (Haine et al., 2015), where it directly influences surface stratification, air–sea heat exchange, and deep water formation in the Greenland Sea (de Steur et al., 2018; Rudels and Quadfasel, 1991). Variability in the EGC freshwater transport can also modify dense water formation and therefore affect the strength of the large-scale Atlantic Meridional Overturning Circulation (AMOC) and its associated climate feedbacks (Le Bras et
50 al., 2021).

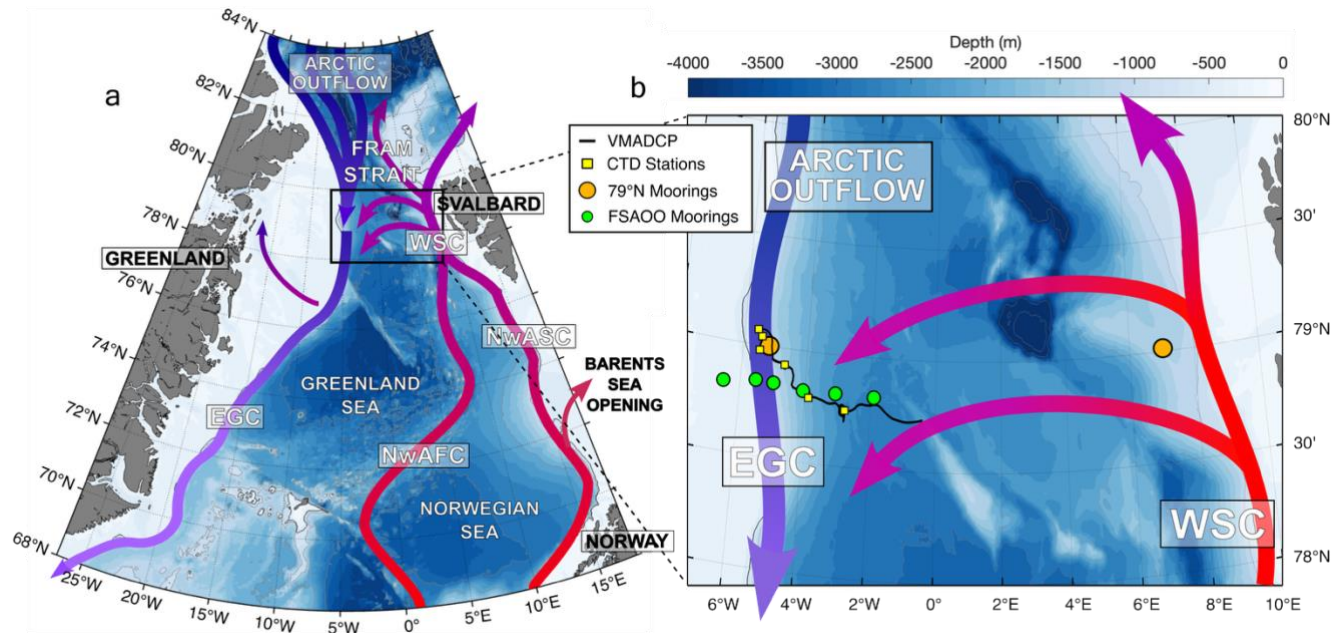
In Fram Strait, the northward-flowing West Spitsbergen Current (WSC) carries warm, saline Atlantic Water (AW) into the Arctic along the eastern side of the strait (Fig. 1) (Aagaard et al., 1987). Approximately half of the AW in the WSC recirculates westward across Fram Strait, subducting
55 beneath the southward-flowing PW (Hofmann et al., 2021; Marnela et al., 2013; Quadfasel et al., 1987) and supplementing the EGC with recirculated AW and Arctic Atlantic Water (AAW) — water of Atlantic origin that has previously circulated through the Arctic Ocean (Rudels, 2002). The westward barotropic recirculation is a part of the large cyclonic wind-driven gyre in the Nordic Seas (de Steur et al., 2014), with its strength and seasonality also eddy-driven (Hattermann et al., 2016), with enhanced
60 eddy kinetic energy originating from baroclinic instability in the WSC which propagates westward (von Appen et al., 2016). The eddies are also considered to facilitate the subduction of AW beneath the sea ice and PW carried southward in the EGC, though the eddy frequency and eddy kinetic energy are much lower in the western Fram Strait and on the East Greenland shelf, where perennial or seasonal sea ice damps surface variability (Bashmachnikov et al., 2020; Hattermann et al., 2016). Part of the recirculated
65 AW is driven onto the Northeast Greenland continental shelf where the Atlantic-origin waters can drive the melting and retreat of the marine-terminating glaciers (McPherson et al., 2024, 2023; Schaffer et al., 2017; Straneo et al., 2012; Wekerle et al., 2024).

The structure and short-term variability of the EGC is characterised as a narrow, topographically steered
70 current concentrated near the shelf-break isobath, embedded in a broader southward flow and interacting with recirculating AW and mesoscale eddies (de Steur et al., 2018, 2014; Håvik et al., 2017). The EGC has shown clear signs of change in its hydrographic properties and freshwater export in recent decades. Long-term observations across the east Greenland continental shelf and slope at 78°50'N, forming the Fram Strait Arctic Outflow Observatory (FSAOO), show significant warming of the upper
75 EGC over recent decades (de Steur et al., 2023). Concurrently, a significant increase in the salinity stratification of the PW due to freshening of the upper layer and increased presence of AW has occurred (Karpouzoglou et al., 2022). Freshwater transport of the EGC is highly variable, driven by changes in



80

EGC volume transport, PW salinity, and the competing influence of AW recirculation, and no long-term trend has been reported up to 2020 (Karpouzoglou et al., 2022).



85

Figure 1: Sketch of the main circulation pathways in (a) the Nordic Seas and Fram Strait, and (b) a close-up of Fram Strait and the measurement locations. Red arrows indicate the northwards flow of warm, saline AW in the West Spitsbergen Current (WSC) in Fram Strait and its westward recirculation. The blue arrow indicates the surface Polar Water and underlying Arctic Atlantic Water, constituting the Arctic Outflow, which feeds the southward flowing East Greenland Current (EGC). The mooring locations considered in this manuscript across the EGC and WSC at 79°N (AWI moorings) are marked as orange circles, the FSAOO (NPI moorings) at 78°50'N are the green circles, the CTD stations are yellow squares, and the vessel mounted ADCP track is the black line.

90

Sea ice export through Fram Strait has declined, primarily as a result of Arctic sea ice thinning rather than changes in ice drift (Spren et al., 2020; Sumata et al., 2023, 2022). The record-low sea-ice export in 2018, however, was a result of both thinner ice together with northward winds that resulted in a longer residence time of sea ice over a warm AW inflow region just north of the Fram Strait (Sumata et al., 2022). Atmospheric forcing — particularly along-slope wind stress and large-scale pressure anomalies associated with the NAO and related patterns — modulates EGC volume and freshwater

95

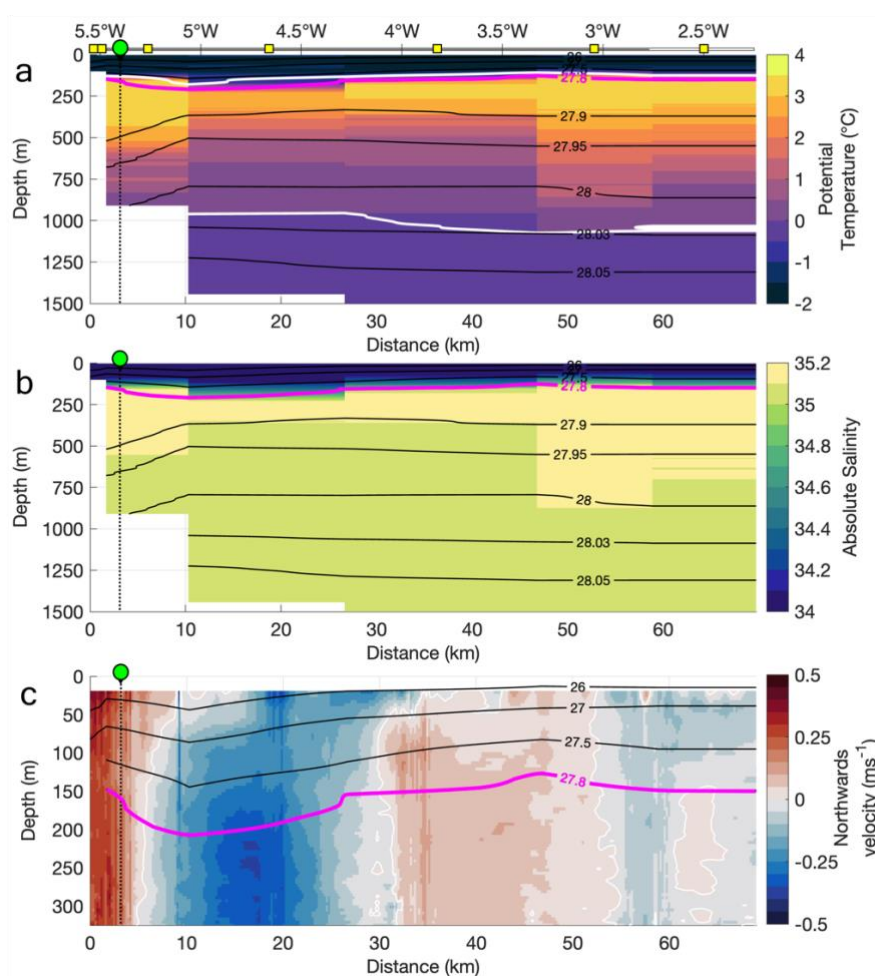
transport on synoptic to interannual timescales, contributing to multi-year anomalies in Fram Strait exchange (de Steur et al., 2018; Håvik and Våge, 2018; Ionita et al., 2016; Karpouzoglou et al., 2024). Taken together, the EGC is becoming warmer and more seasonally stratified in its upper layers, with increasing AW influence at depth, as well as much thinner and less sea ice coverage since 2007. Its variability reflects the interplay of a changing Arctic, variable Atlantic inflow, and strongly modulating atmospheric forcing.

100

In this study, we present seven years (2018–2025) of continuous mooring observations from the East Greenland continental slope at 79°N, alongside hydrographic and velocity sections. The observations



105 reveal a number of northward flow events in the EGC - contrary to the general southward direction of
the boundary current - which spanned a range of durations and vertical structures. Two of these events
— in April–May 2019 and May–June 2025 — are anomalous in their duration, intensity, and vertical
coherence (reaching down to 500m depth), and will be the focus of this study. Using complementary
data from the FSAOO mooring array at 78°50'N, approximately 18km south of the 79°N mooring, we
examine the hydrographic signature of these northward flow events, the atmospheric and dynamical
110 forcing responsible for them, and their lateral extent across the continental slope. We further assess their
implications for the anomalous transport of Atlantic heat into the Arctic interior and for regional sea ice
variability, and consider whether such events represent rare features of a naturally variable boundary
current or early signals of ongoing change in the Arctic-Atlantic exchange.



115 **Figure 2.** Vertical sections of (a) potential temperature, and (b) absolute salinity, from the CTD sections, and (c) northward
velocity along the ship track (black line in 1b) (positive velocities are northward) from the VMADCP (note that the vertical range
in c is much shorter than in a/b). The thin labelled contours are potential density (kg m^{-3}) and the bold magenta contour is the 27.8
120 kg m^{-3} isopycnal. The white contours represent (a) the 0°C isotherm and (c) 0 ms^{-1} . The section distance is 0 km at the east
Greenland shelf (the westernmost point of the ship transect). The location of the 79°N mooring (green circle) and CTD profiles
(yellow squares) are marked at the top of (a).



2 Methods

2.1 Mooring arrays

To monitor the year-round oceanic exchange of heat, freshwater and sea ice across Fram Strait, the
125 Alfred Wegener Institute, Helmholtz Centre for Polar and Marine Research (AWI), and the Norwegian
Polar Institute (NPI) have been maintaining a mooring array spanning the strait since 1997. The array
provides hydrographic and current velocity data, as well biological and biogeochemical parameters,
from both the WSC (AWI) in the east (McPherson et al., 2026) and the EGC (NPI) in the west. While
NPI has led the effort in monitoring the EGC at 78°50' N with the Fram Strait Arctic Outflow
130 Observatory (FSAOO) (de Steur et al., 2023), AWI has maintained one mooring on the continental shelf
of eastern Greenland at 79°N since 2018 (~1000m water depth), referred to here as the 79°N mooring.

The 79°N mooring was most recently deployed at 79°N, 5°23.8'W during cruise PS143.2 of RV
Polarstern (July–August 2024; Metfies, 2025) and recovered on 16 June 2025 during PS148 (Dannheim,
135 2025) (Fig 1b). The mooring configuration has been maintained continuously since 2018, with current
meters (Seaguard or RCM11, depending on the year) at nominal depths of 50 m (targeting the cold,
fresh PW surface layer), 250 m (the warm, saline AW layer, recirculated westwards from the WSC),
and 500 m (the Arctic Atlantic Water that has recirculated through the Arctic and is exported through
Fram Strait), with SBE37s measuring temperature and salinity approximately 5 m above each current
140 meter (Appendix Table 1).

An additional AWI mooring was deployed during PS143.2 (17 July 2024) in eastern Fram Strait at
79°0.7'N, 7°2.1'E (Fig. 1b), located in the offshore branch of the AW inflow that forms the WSC. At
250 m, in the AW layer, an SBE37 CTD measured temperature and salinity every 10 minutes. The
145 mooring was also recovered during PS148 on 22 June 2025. Full details of the WSC mooring array are
given in McPherson et al., (2026).

The FSAOO mooring array has been maintained in the EGC at 78°50'N since September 2003, while
between 1997-2002 it was located at 79°N. This array consists of 6 moorings spanning the continental
150 shelf in 225m water depth (8°W), the continental slope (from ~2450m, 1850m, 1030m, 270m at 3°W,
4°W, 5°W and 6.5°W resp.) and into central Fram Strait (~2670m, 2°W) (Fig. 1b). They measure
temperature and salinity (SBE37, RBR CTD) and velocities (ADCPs, RCMs, Aquadopps) from the
near-bottom to 50-m subsurface, as well as sea-ice draft and sea-ice velocity (Spreen et al., 2020;
Sumata et al., 2022). More details about the oceanographic data collected by the moorings can be found
155 in de Steur et al., (2018) and Karpouzoglou et al., (2022). The temperature and velocity data across the
FSAOO mooring array used in this analysis is from September 2003 - August 2019 and has been
monthly averaged and gridded (Karpouzoglou et al., 2021).

All measurements from the 79°N mooring were daily averaged to a common time series. A deep-
160 reaching northward event in the EGC is defined as when the v-component of the measured velocities at
all three 79°N mooring instrument depths (50/250/500m) is northwards (i.e., $v > 0$ ms⁻¹). A local event



is defined as when the v-component of at least one of the three depths is northwards. The absence of velocity measurements below 500 m means that these events cannot be confirmed as full-depth barotropic events — extending to the seabed at ~1000 m.

165 **2.2 Ship-based CTD and ADCP data**

During PS148, eight hydrographic profiles of conductivity-temperature-depth (CTD) were collected across the eastern Greenland continental shelf, spanning the continental shelf towards central Fram Strait and including at the mooring location (Fig. 1b). The CTD casts were recorded with a dual duct Sea-Bird 911+ and averaged into 1 m bins. Conductivity and oxygen sensors were calibrated using
170 water samples analysed on board with an Optimare Precision salinometer and titration, respectively.

A vessel-mounted ADCP (150 kHz RDI Ocean Surveyor ADCP, VMADCP) recorded ocean velocities along the cruise track during PS148. The VMADCP recorded velocity in 4 m bins over the depth range from approximately 15 m from the surface to approximately 300 m. The VMADCP data was processed
175 with the Ocean Surveyor Sputum Interpreter software, version1.9, developed by GEOMAR.

2.3 Sea Ice Data

Daily mean sea ice concentration since 2003 were calculated from the 89 GHz channels of the AMSR satellite microwave radiometer series (Sprenn et al., 2008) and obtained on a 6.25 km grid from the University of Bremen (www.seaice.uni-bremen.de). Sea ice concentration for the region of interest
180 79°N – 85°N, 25°W – 5°E were obtained by averaging the grid cells within that region. Uncertainties are usually within ±5% for high ice concentration. However, during summer melt ponds can cause an underestimation larger than that.

Sea ice motion data were obtained from the Ocean and Sea Ice Satellite Application Facility (OSI SAF).
185 The OSI-405-c drift product (Lavergne, 2016) is provided on a daily basis at a spatial resolution of 62.5 × 62.5 km. The product resolves large-scale and synoptic variability in Arctic sea ice drift (Krumpen et al., 2020), but tends to underestimate drift speeds in coastal regions and in narrow straits such as Fram Strait (Krumpen et al., 2021).

2.4 Atmospheric Data

190 Monthly and daily mean sea level pressure and surface wind fields were obtained from the fifth generation European Centre for Medium-Range Weather Forecasts (ECMWF) atmospheric reanalysis (ERA5; Hersbach et al., 2020). The dataset provides global coverage on a regular latitude–longitude grid (0.25°X 0.25°) and is available from the Copernicus Climate Change Service (C3S) Climate Data Store.

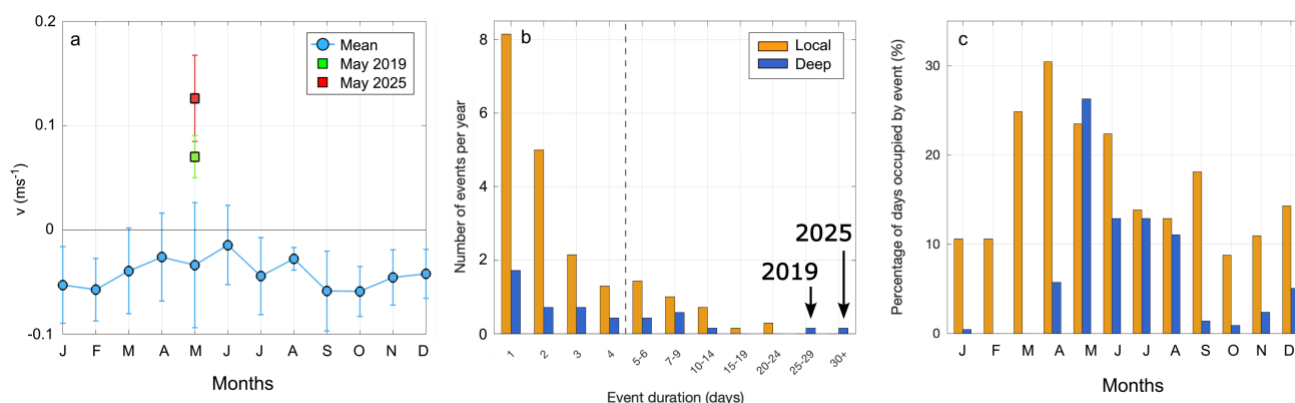


195 3 Results

3.1 Observations of Anomalous Northwards Flow

Typically, the 79°N mooring between 2018–2025 captures a persistent, year-round southward flow ($v < 0 \text{ m s}^{-1}$) over the upper 500m (Fig 3a). This southward flow is strongest between autumn and winter (the absolute value is larger than 0.05 ms^{-1}), consistent with the intensified wind stress over the Nordic Seas over these months which spins up the gyre circulation (Isachsen et al., 2003; Voet et al., 2010), resulting in stronger southwards velocities in the EGC in winter (de Steur et al., 2014).

A number of ‘reversals’ of the current were observed, where either part of, or the full upper 500m, was marked by a northward velocity. Approximately 85% of all observed northward events during this period were local northward flow events which we define as times when northward flow ($v > 0 \text{ ms}^{-1}$) is recorded at at least one, but not all, of the three observed depths. These local events are typically subsurface intensified and over 80% of them lasted fewer than 5 days. That is, the majority of them may lie within the typical timescale of mesoscale eddies in the region (Wekerle et al., 2020), though two local events last between 20 - 25 days (Fig. 3b). These local events occurred year-round but showed a seasonal bias, occurring most frequently in spring in over 20% of days in March - June, and least frequently during autumn, in $< 15\%$ days during October - February (Fig. 3c).



215 **Figure 3. (a) Seasonal cycle of upper 500m northward velocities (calculated as the mean of the velocities at 50m, 250m, 500m) at 79°N between 2018 - 2025 with May 2019 and May 2025 removed (blue). The mean northward velocities in May 2019 and May 2025 are marked by the green and red squares. Whiskers represent the standard deviation. Histograms of (b) number of events per year between 2018 - 2025 by duration, and (c) the percentage of days in each month that local (i.e., when at least one of the depths shows a northwards/v-positive flow; orange) and deep (when all three depths show a northwards/v-positive flow; blue) events occur. The dashed line in (b) is at 5 days, marking the typical timescale of mesoscale eddies in the region, and the two longest deep northward events are labelled with the year in which they occurred.**

Deep-reaching northward events (i.e., when the flow at all three measured depths is northwards; $v > 0 \text{ ms}^{-1}$) were much less frequent, accounting for only $\sim 15\%$ of all events. Seasonally, these deep events were also concentrated in spring and summer, occurring in over 10% days through May to August, and less than 5% of days in autumn and winter (September - March). The strong springtime bias of northward events suggests a potential role for seasonal forcing mechanisms. Generally these events

have been similarly short-lived, with 75% lasting less than 5 days (Fig. 3b), with a typical mean northward velocity of $0.04 \pm 0.06 \text{ m s}^{-1}$. The strongest northward velocities typically occurred at 250m and reduced magnitude at 500m depth, reflecting substantial vertical shear (Fig. A1).

230 Two deep events deviated substantially from this typical pattern of short-lived events: a 29-day event in
May 2019 (25 April to 23 May), and an (at least) 35-day event in May 2025 (4 May - 16 June); note that
the latter event was ongoing when the mooring was recovered which is why we cannot determine
exactly how long it lasted. These events lasted nearly three times longer than any other deep-reaching
event in the record. The 2025 event was markedly more intense, with a mean northward velocity in May
235 2025 of $0.13 \pm 0.04 \text{ m s}^{-1}$ - more than twice as fast as May 2019 ($0.07 \pm 0.02 \text{ m s}^{-1}$) (Fig 3a) and
other deep events ($0.04 \pm 0.03 \text{ m s}^{-1}$). This combination of exceptional duration, intensity and vertical
coherence marks the May 2025 event as an unprecedented event in the 2018–2025 mooring record.

Historical observations from a mooring of the FSAOO between 1997–2002 (F13, also at 79°N during
240 that period, but at 5.3°W ; $\sim 2 \text{ km}$ from our mooring sites) provide more context of this anomaly. Mean
meridional velocities during that period were southward, measured as $-0.04 \pm 0.06 \text{ m s}^{-1}$ at 50 m and
 $-0.01 \pm 0.04 \text{ m s}^{-1}$ at 240 m (de Steur et al., 2014). In contrast, the May 2025 event exceeded these
historical means by more than two standard deviations, placing the 2025 event well outside the expected
range of variability and further underscoring its extreme character in the context of both recent and
245 longer-term observations.

3.2 Hydrographic Structure during Northward Flow Events

The 2019 and 2025 northward events, by virtue of their exceptional duration and intensity, provide the
clearest opportunity to examine the hydrographic and dynamical character of anomalous northward
flow in the EGC, and form the focus of the remaining analysis.

250 The hydrographic section collected across the East Greenland continental shelf break near 79°N in June
2025 shows a classic three-layered structure of the EGC, consistent with previous observations (e.g.,
Håvik et al., 2017). The surface layer consists of cold, fresh Polar Surface Water (PSW) extending
across the entire section and reaching depths of $\sim 150\text{m}$ over the slope (Fig. 2a,b). Below the PSW is the
255 $\sim 600\text{--}850\text{m}$ thick layer of Atlantic-origin water, broadly defined as temperatures $> 0^\circ\text{C}$. This layer
comprised two distinct components: the warm and saline Atlantic Water (AW) that originates directly
from the West Spitsbergen Current (WSC) and has recirculated in Fram Strait, which sits atop the
colder, fresher Arctic Atlantic Water (AAW) typically found along the eastern Greenland slope (Rudels,
2002). Below the deep 0°C isotherm at $\sim 1000\text{m}$, the lower intermediate layer was colder and less saline.
260 The velocity structure across the section at the time of the mooring recovery shows that the strong
northwards flow sits on the continental shelf break, with the mooring located on its eastern edge (Fig
2c). The flow was barotropic out to 5 km from the shelf edge and peaked in the near-surface at 0.4 m s^{-1} .
This northwards flow was supported by the density front of upwards sloping isopycnals rising toward
the Greenland shelf in the upper 300m, indicating a reversal of the typical baroclinic structure of the
265 boundary current. While there is no VMADCP data below 300m, the mooring record shows the



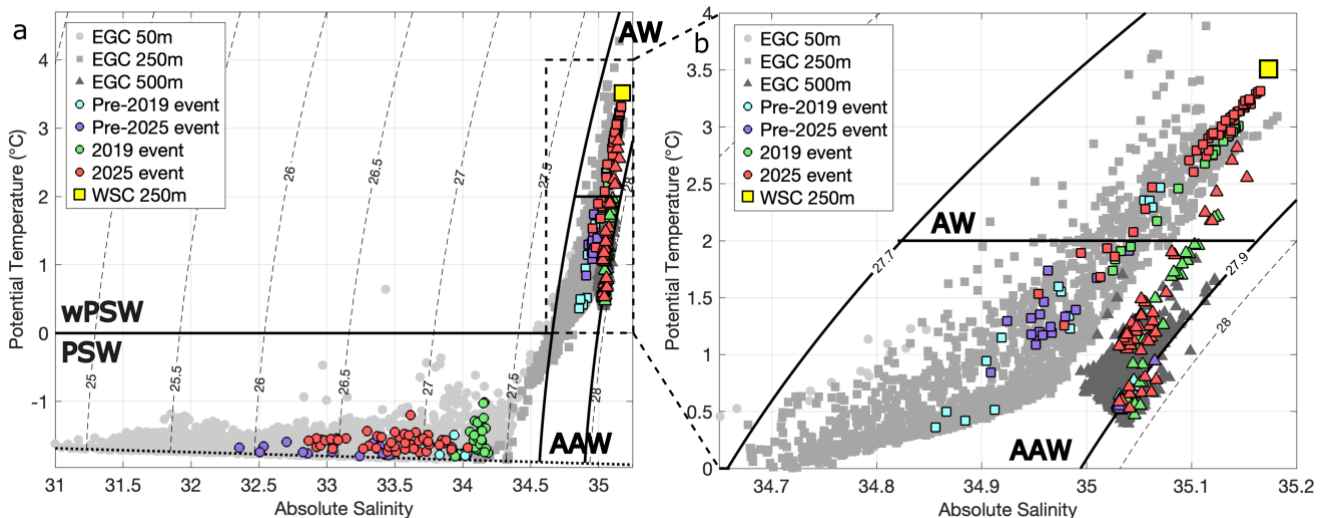
northward flow reached at least down to 500 m (Fig. A1). Below 500m, the isopycnals slope downward toward the coast. If the flow is dynamically consistent with the hydrographic structure, this reflects a return to the typical long-term mean baroclinic structure of the EGC where deeper, denser layers are flowing southward in geostrophic balance (Håvik et al., 2017; Karpouzoglou et al., 2022).

270 Unfortunately, there is no velocity data below 500m to check if the flow deeper in the water column was also northward.

To the east of the northward flow, a well-defined strong southwards flow extended 30 km offshore from the continental shelf edge, with a subsurface-intensified core reaching over 0.4 ms⁻¹ below 200 m (Fig. 2c). It is supported by the shoaling in the offshore direction of isopycnals in the upper 500m. The characteristics of the current here are consistent with the estimates of width and core speed of the shelfbreak EGC that Håvik et al., (2017) defined as the most prominent component of the boundary current system. Immediately offshore of the strong southward core, the flow was weaker and at times northward, suggestive of eddies likely formed via baroclinic instability of the boundary current (Håvik et al., 2017).

275

280



285 **Figure 4. Potential temperature–Absolute salinity (T/S) diagrams at 50 m (light grey), 250 m (medium grey) and 500 m (dark grey) at the EGC mooring location from 2018 - 2025. The T/S properties during the 2019 and 2025 events at each depth are green and red respectively, and the cyan and purple are the T/S properties over the 2 weeks before the 2019 and 2025 events. The dots are daily means from the individual instruments. The yellow square is the mean T/S properties from the offshore branch of the WSC at 250 m, from the 2024 - 2025 mooring deployment. Contours are selected isopycnals (kg m⁻³) and the freezing line is the dotted black line at the bottom. Acronyms are water masses defined by Rudels et al (2000); warm Polar Surface Water (wPSW), Polar Surface Water (PSW), Atlantic Water (AW), and Arctic Atlantic Water (AAW).**

290 The May 2019 and 2025 northward flow events were also associated with changes in the hydrographic structure, as shown by temperature–salinity (T-S) properties at the three measured depths (50 m, 250 m, 500 m) compared to the 2018–2025 mooring observations at the site. In the PSW layer at 50 m, the temperature properties were not highly anomalous during the 2019 and 2025 events (Fig. 4). Mean temperatures matched the long-term May average (-1.7°C), while salinity was slightly elevated,



295 particularly during the 2019 event (mean of 34.1 and 33.5 for the 2019 and 2025 events compared to a
climatological mean of 32.8) (Fig. A2). At 250m however, the water mass properties during the events
were much warmer than usual, with mean temperatures of 2.8°C and 2.7°C respectively compared to a
climatological May mean of 1.2°C, and similar salinities of ~35. This indicates a clear dominance of
300 AW during both events, while colder AAW was typically present at this depth. A similar pattern was
observed at 500 m, where mean temperatures during the events (1.4°C and 1.3°C in 2019 and 2025
respectively) exceeded the climatological May average (0.7 °C), suggesting the presence of deep and
warm AW that has extended below the usually AAW dominated layer.

305 This close agreement in T-S properties between the 2019 and 2025 events — anomalously warm and
saline at 250m and 500m, with AW dominating at depths typically occupied by AAW, and near-typical
PSW properties at 50m — suggests that both events involved the same physical process: a subsurface
intrusion of Atlantic-origin water coinciding with the northward event. While the 2025 event was
exceptional in its duration and intensity relative to the full mooring record, the hydrographic similarity
with 2019 indicates that this class of northward event, characterised by anomalous AW presence at
310 depth, is not unique.

In the two weeks preceding both events, salinities and temperatures were generally typical of the mean
properties for the EGC at each depth, though near-surface salinities in 2019 were slightly higher. This
suggests that the EGC was hydrographically typical and stratified as expected up until both events, with
315 no anticipatory signal in water mass properties. These abrupt shifts in T-S properties are consistent with
a rapid response to external forcing (e.g., wind stress, eddy passage, or barotropic pressure anomalies)
rather than a gradual change in the physical properties.

320 The mooring data also shows that vertical stratification in the upper layers weakened during the two
major deep-reaching events. During the whole record, the stratification (N^2) between the PSW and the
AW/AAW interface calculated between the instruments at 50 m and 250 m was around $N^2 =$
 $8 \times 10^{-5} \text{ s}^{-2}$. During the 2019 and 2025 events, however, this dropped to about $3 \times 10^{-5} \text{ s}^{-2}$ and
 $5 \times 10^{-5} \text{ s}^{-2}$ respectively, reflecting a reduced vertical density gradient. Since the T-S properties at 50m
remained within the historical mean, while those at 250m were anomalously warm (Fig. 4), this
325 suggests the stratification weakened resulting from the presence of anomalous subsurface water mass —
likely associated with an intrusion of Atlantic-origin waters — rather than from enhanced vertical
mixing or convection. Between 250m and 500m, the stratification remained fairly unchanged.

330 The origin of this intruding AW can be inferred from the T-S properties at 250m. The hydrographic
properties of the EGC at this depth are generally colder than the AW found in the offshore branch of the
West Spitsbergen Current (WSC) (Fig. 4). During the May 2025 northward event, however, the
warmest and more saline T-S properties at 250 m in the EGC approached those of the AW in the WSC,
both falling along the same isopycnal. This alignment suggests that the AW responsible for the
weakened stratification in the EGC, was recently derived from, or directly influenced by, the WSC,
335 consistent with westward recirculation across Fram Strait (Hofmann et al., 2021; Marnela et al., 2013;
McPherson et al., 2023; Quadfasel et al., 1987). Notably, AW in the offshore branch of the WSC in

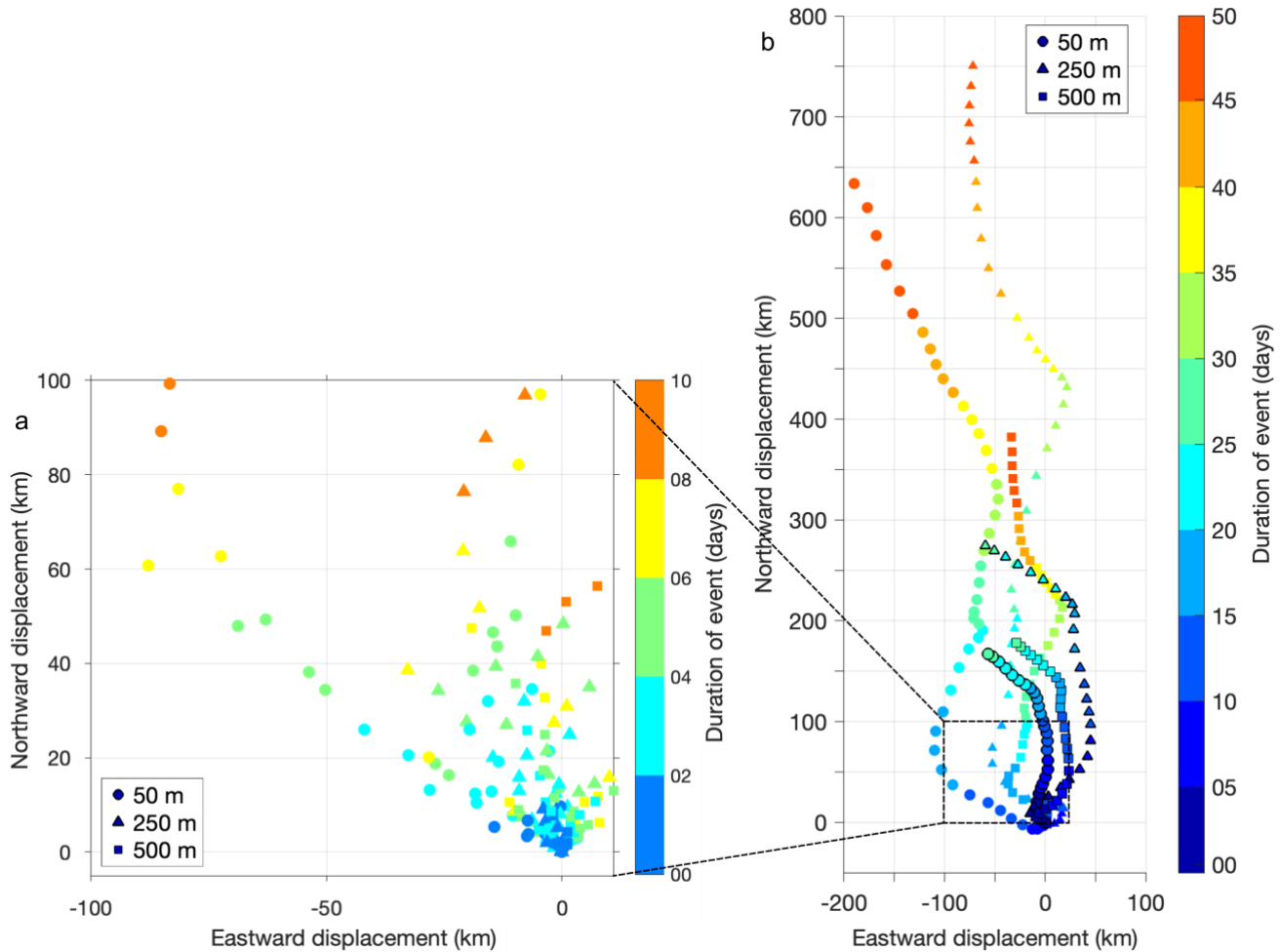
eastern Fram Strait occupies a similar depth range of 400–500 m (McPherson et al., 2026), suggesting that the anomalously warm water observed at 500 m in the EGC during both events lies on the same depth horizon as its likely source, consistent with direct lateral advection of AW across Fram Strait at this density level rather than vertical displacement within the water column. The convergence of T-S properties and isopycnal structure suggests that the anomalous northward flow in the EGC coincided with either an enhanced westward intrusion of AW directly from the WSC recirculation, or AW was displaced northward from its typically more southern meeting point with the EGC near 78° 50'N (de Steur et al., 2014). The available hydrographic observations cannot distinguish between these two pathways, as both would produce similar T-S signatures at the mooring location.

3.3 Spatial Extent of Northward Flow Events

To assess the spatial extent of the major northward events, we examine both the potential northward advective reach and the lateral extent of the forcing using data from the FSAOO mooring array at 78°50'N.

Progressive vector diagrams for all deep northward events lasting more than 5 days — excluding the exceptional 2019 and 2025 events — show maximum northward displacements of approximately 80–100 km, with most events reaching less than 50 km (Fig. 5a). These displacements, even for events with a smaller magnitude and duration, are sufficient to transport anomalous water masses — particularly PSW at 50m and AW at 250m, which show the largest displacements — beyond the immediate mooring location, suggesting that the cumulative effect of recurring shorter northward events may impact the mean hydrographic state of the upper EGC over seasonal timescales.

Progressive vector diagrams for the 2019 and 2025 events show sustained northward displacement at all measured depths, with the largest displacements occurring at 250m where warm AW was present (Fig. 5b). Note that the scale differs substantially between the two panels — the 2019 and 2025 events produce northward displacements an order of magnitude larger than any other event in the record. These diagrams assume that water parcels observed at the 79°N mooring continued northward at the measured velocity; we do not suggest that this would have happened, but use the diagrams to establish an order of magnitude. The progressive vector diagrams therefore represent an upper bound on advective reach rather than a confirmed trajectory. Under this assumption, subsurface AW at 250m could have been advected approximately 250 km northward during the 2019 event, reaching ~81°N, and over 750 km during the 2025 event, potentially reaching ~86°N. The greater northward extent in 2025 reflects its longer duration rather than substantially stronger velocities, as both reach a similar northwards distance within the first 20 days. These estimates highlight the potential for such northward events to transport anomalously warm Atlantic-origin waters considerable distances northward into the Arctic, with significant implications for sea ice and upper Arctic ocean heat content, which we explore in the following section.



375 **Figure 5. Progressive vector diagram of the velocities from (a) all the deep-reaching northward events than lasted over 5 days, excluding 2019 and 2025, and (b) the 2019 (outlined) and 2025 events at 50m (circles), 250m (triangles), and 500m (squares). Note the scales differ between the two panels.**

To assess the lateral structure of the 2019 northward flow event, data from the FSAOO mooring array at 78°50'N, approximately 18 km south of the 79°N mooring, was examined. The array spans the continental shelf, shelf-break, and slope between the ~270m and ~2650m isobaths. The long-term May mean temperature section (Fig. 6a) shows the classic hydrographic structure of the EGC consistent with observations at 79°N (Fig. 2a), with a well-defined AW core with temperatures greater than 2°C centred between 2 - 3°W at depths of 200 - 400 m. The long-term May mean velocity section shows a consistent southward flow across the width of the mooring array (Fig. 6d). The EGC core is clearly visible with the strongest southward flow exceeding 0.1 ms⁻¹ and surface-intensified, centred between 2°W and 4°W. Note that at 78°50'N, the flow is more barotropic in character than at 79°N attributed to the (strongly seasonally varying) westward recirculation of AW from the WSC across Fram Strait (Fig. 1a),

380

385

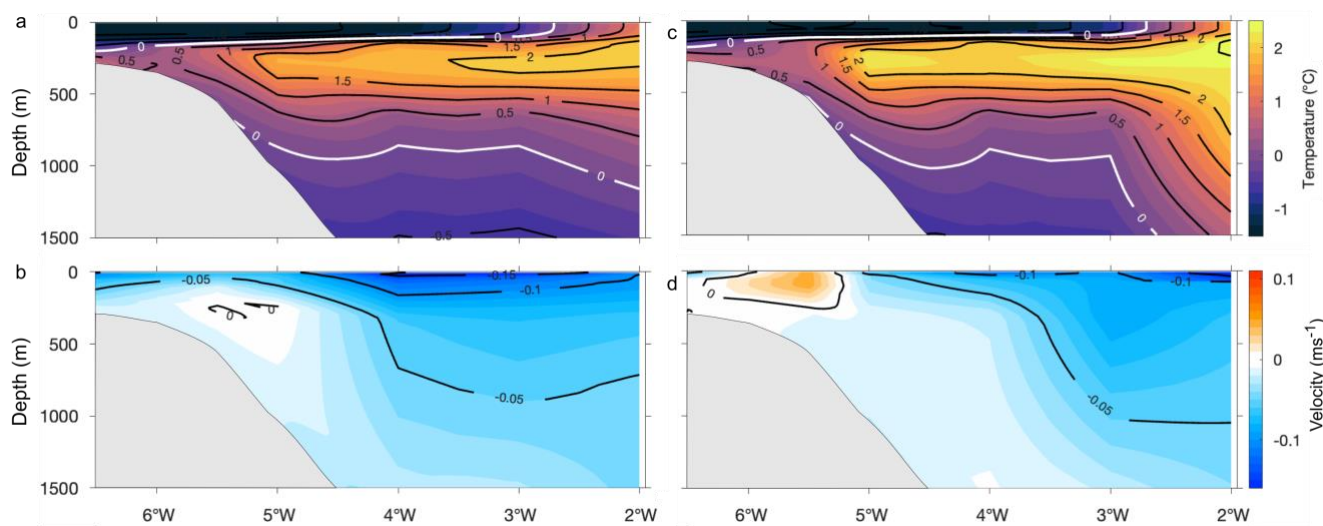
which modifies the density structure and vertical shear of the current at this latitude (de Steur et al., 2014).

390

During May 2019, the FSAOO temperature section (Fig. 6c) reveals a warmer AW core relative to the long-term May mean (Fig. 6a), with the 2°C isotherm extending further inshore and the subsurface AW layer appearing warmer. This subsurface warming at 78°50'N is consistent with the anomalously warm AW observed simultaneously at the upstream 79°N mooring during the event (Fig. 4), suggesting that the AW intrusion associated with the northward flow event was a spatially coherent feature extending across at least 18 km of the East Greenland margin. Northward flow during the 2019 event was confined to the inshore part of the array around 5°W–6°W in the upper ~200m (Fig. 56), with no complete velocity reversal observed at any other mooring location, indicating that the northward flow was laterally confined to a narrow band of not more than 30 km width along the continental shelf-break. There was no detectable lag in the velocity records for the timing of the event at 78° 50'N and 79°N which indicates that the forcing acted coherently across both latitudes.

395

400



405

Figure 6. Average May sections of (top) potential temperature and (bottom) northward velocity (a,b) between 2003 - 2019 and (c,d) over May 2019 across the FSAOO mooring array at 78°50'N.

410

415

Whilst the northward velocity itself was confined to the shelf-break, the velocity structure across the array does reveal a wider footprint of change in the EGCs structure across the continental slope. Comparing the May 2019 velocity (Fig. 6d) with the long-term May mean (Fig. 6b), there is a clear offshore displacement of the EGC core, where southward velocities exceed 0.1 m s⁻¹, from its mean position between 2°W and 4°W in the upper 200m to east of 3°W during May 2019. Between the northward flow at the shelf-break and the displaced core, southward velocities were substantially weaker than the long-term mean, with the 0.05 m s⁻¹ contour retreating offshore and near-zero velocities occupying much of the upper mid-slope region around 4°W–5°W. Importantly, this weakening extends through the water column across the mid-slope rather than being confined to the surface layer, indicating that the northward forcing was vertically coherent across the upper slope rather than just a



420 surface-driven response. This pattern, combined with the northward signal at the shelf-break, is consistent with a coherent northward forcing acting across the full width of the continental slope to at least the ~2500m isobath, a lateral distance of approximately 80 km from the shelf-break. Farther offshore toward the central Fram Strait, the surface-intensified southward flow at 2°W was maintained and slightly intensified relative to the mean, consistent with an offshore shift of the boundary current.

425 Whilst the analysis above focuses on the 2019 event during the overlap period between the two mooring records, the full FSAOO dataset between 2003 - 2019 reveals that northward flow events at the shelf-break are a recurring feature at 78°50'N. A total of 8 deep-reaching northward flow events were identified over this period, occurring predominantly in late spring and summer. Two particularly strong events stand out — in June 2004 and February 2008 — when northward velocities on the shelf-break and upper slope exceeded 0.15 m s⁻¹. The June 2004 event is notable for its spatial extent, with northward flow extending to approximately 750 m depth and between 4°30'W - 6°15'W (Fig. A3) — substantially broader, deeper and faster than observed in May 2019 (Fig. 6b). The AW temperature anomaly at the shelf-break, calculated relative to the monthly climatology, is also generally positive during these 8 deep-reaching northward flow events (Fig. A4), consistent with the northward advection of anomalously warm AW documented at 79°N during the 2019 and 2025 events. In May 2019, a comparatively small temperature anomaly at 78°50'N is consistent with its weaker northward velocities relative to the 2004 and 2008 events.

435 It should also be noted that the 78°50'N dataset consists of monthly means, which precludes direct comparison of event duration with the daily-resolution 79°N record, and may underestimate instantaneous velocities during individual events. Nevertheless, the occurrence of recurring northward flow events across more than two decades, including events of greater intensity than those captured in the 2018-2025 record at 79°N, establishes that episodic northward flow is an intrinsic feature of the EGC system at the East Greenland shelf-break rather than a recent phenomenon.

4 Possible Drivers of Anomalous Northward Flow

4.1 Eddies

445 Mesoscale and submesoscale eddies play a critical role in shaping the hydrography and dynamics of Fram Strait, modulating short-term variability in the EGC through episodic pulses of heat, salt, and momentum (Wekerle et al., 2020). Eddies are generated primarily by baroclinic instability of the strong lateral density gradients between warm, salty AW and cold, fresh Polar Water (PW) and Arctic outflow, and are winter-intensified as a result of strong atmospheric cooling (von Appen et al., 2016). As eddies pass the mooring, they could drive a transient northward flow signal. Eddy kinetic energy in Fram Strait is concentrated in the eastern and central strait along the WSC and AW recirculation (von Appen et al., 2016; Wekerle et al., 2020), with significantly lower values on the western shelf-slope where the EGC resides (Jónsson et al., 1992). While westward-propagating eddies from the eastern strait occasionally

interact with the EGC, they do not generally constitute a sustained eddy field at the shelf-break, making it unlikely that eddy passage alone could drive the prolonged, vertically coherent event observed here.

455

To assess whether eddy passage could account for the prolonged deep-reaching northward events, the spatial scale an eddy would need to produce a continuous unidirectional signal of the observed duration at the mooring can be estimated. The required eddy diameter can be estimated as the product of the mean observed deep northward velocity and event duration, assuming the eddy is advected past the mooring at the mean northward velocity. For the 2019 event with a mean velocity of 0.07 ms^{-1} over the 29 days, this equates to a diameter of approximately 175 km and equivalent radius of $\sim 88 \text{ km}$. For the 2025 event (mean velocity 0.13 m s^{-1} over (at least) 35 days) yields a diameter of approximately 393 km and thus radius of $\sim 197 \text{ km}$.

460

465 These scales are between one to two orders of magnitude larger than both the Rossby radius of deformation in Fram Strait which characterises the spatial scale of eddies (4–6 km in summer; von Appen et al., (2016) and the observed eddy size distribution, in which over 90% of eddies have radii below 10 km (Wekerle et al., 2020). Even accounting for uncertainty in eddy propagation speed, it is highly unlikely that an eddy of this scale could occur and sustain the observed northward signal for the duration of either event. It is also worth noting that northward events in the EGC have been documented elsewhere along the east Greenland margin. de Steur et al., 2017 described an energetic reversal of the shelfbreak EGC at 68°N , i.e. north of Denmark Strait, in November 2011 which persisted for nearly a month and was attributed to the passage of a large anticyclone. It was explicitly noted that a feature of this scale (order $\sim 100 \text{ km}$ diameter) was unlikely to have formed via baroclinic instability of the current, which would tend to generate smaller eddies of order 25–50 km, and suggested instead that anomalous wind stress curl during October may have played a role in its generation. Notably, even an anticyclone of this scale ($\sim 100 \text{ km}$ diameter) would be inconsistent with the lateral confinement of the northward flow at 79°N to a band of no more than 30 km width (Fig. 2c), further excluding eddy passage as a viable explanation regardless of the eddy's size or origin.

470

475

480

While this demonstrates that large-scale, wind-influenced events can occur within the wider EGC boundary current system, there are a number of factors that distinguish that event from the prolonged deep northward flow events documented here. The November 2011 event occurred considerably further south, near Denmark Strait, and mean velocities over the upper 155m across the NPI section at $78^\circ 50'\text{N}$ were consistently southward in 2011 (Karpouzoglou et al., 2022). The November timing further south is also different from the northward flow events seen in April-May-June identified in the 79°N mooring record (Fig. 2c). The Denmark Strait event therefore represents a distinct and different class of event, and whilst the role of wind forcing in both cases suggests a possible common atmospheric influence on northward flow along the Greenland continental slope more broadly, the mechanisms and scales involved differ substantially from those described here. Mesoscale eddies thus contribute to the short-lived baroclinic variability that characterises the majority of northward events in the record (Fig 2b) — whose 4–10 day timescales are consistent with typical eddy lifetimes in the region. However, they cannot plausibly account for the duration, vertical coherence, or spatial extent of the prolonged 2019 and 2025 events on either energetic or geometric grounds.

485

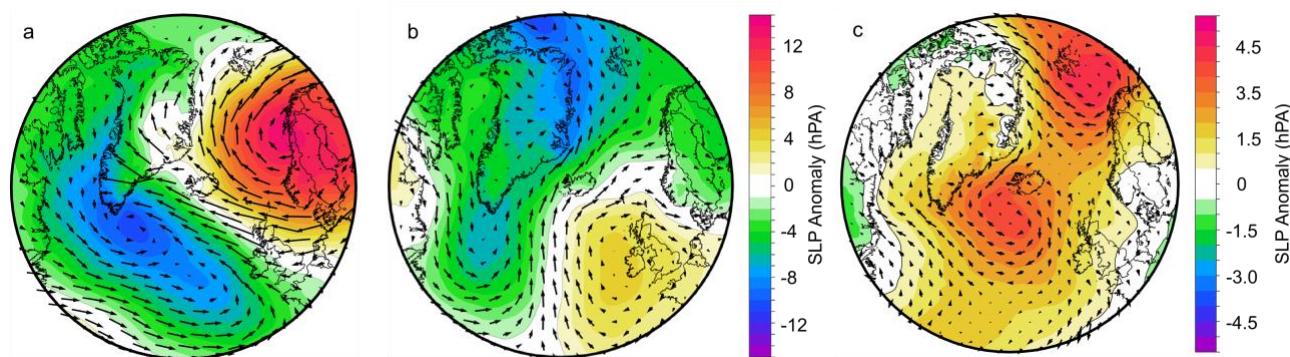
490



495 4.2 Atmospheric Forcing

Atmospheric forcing — particularly sustained wind stress associated with large-scale pressure anomalies — has long been recognised as a major driver of EGC variability across timescales from days to interannual (de Steur et al., 2014; Håvik and Våge, 2018; Karpouzoglou et al., 2024; Smedsrud et al., 2017). Anomalous depth-uniform reversal events in boundary current systems are often attributed as
 500 barotropic responses to local wind forcing or remote barotropic pressure anomalies (Sutherland and Pickart, 2008; Woodgate et al., 1999). Here, we investigate the atmospheric forcing during the deep events in order to determine the dynamical pathways that drive the observed oceanic response.

During May 2025, large-scale sea-level pressure (SLP) anomalies exhibit a pronounced dipole structure,
 505 with anomalously high pressure over the North Atlantic and the British Isles and anomalously low pressure over Greenland (Fig. 7b). This pressure gradient drives a strong and sustained northward wind anomaly along the East Greenland continental shelf and through Fram Strait. In April 2019 - the month in which the 2019 deep northward flow event began - a largely similarly positioned anomalous pressure gradient largely reduced the prevailing southward winds over the western Fram Strait (Fig. 7a), rather
 510 than a full reversal to northward winds as observed in May 2025. Notably, the monthly mean wind anomaly for May 2019 — when the 2019 event was ongoing — had a weakening northward wind signal relative to April, suggesting that the atmospheric forcing may have been waning whilst the oceanic northward flow persisted. Similarly, the wind anomalies by the first week of June 2025 had also
 515 weakened (not shown), despite the persistent northward oceanic flow. This suggests the boundary current system does not have a direct and immediate response to instantaneous wind stress but rather reflects the inertia of a geostrophic adjustment process.



520 **Figure 7. Maps of anomalous sea level pressure (SLP) and surface wind fields (arrows) at 10 m height averaged over (a) April 2019, (b) May 2025 and (c) composite map of all anomalously strong deep northward events over the upper 500m at the 79°N EGC mooring location (Fig. A2).**

A composite of all anomalously strong deep northward events in the 2018 - 2025 record, defined as the average 500m velocities stronger than 1 standard deviation from the mean (Fig. A2), reveals a broadly similar northward wind pattern through Fram Strait (Fig. 7b). However, the composite wind anomalies
 525 are of weaker magnitude than those observed in May 2025, and are associated with a somewhat



different large-scale SLP structure in both sign and spatial distribution. The composite signal therefore reflects a tendency across multiple events rather than a universal forcing pattern, and the 2025 event remains the most strongly atmospherically forced case in the record.

530 Together, these results suggest that northward wind forcing anomalies, whether largely weakened
prevailing southward winds or a full reversal, along the East Greenland margin are a recurring
dynamical feature associated with deep northward flow events, rather than a phenomenon unique to
2025. Whilst the initial barotropic oceanic response to wind forcing adjusts on timescales of hours to a
few days, the persistence of the northward flow into May 2019 after the northward wind anomaly had
535 weakened relative to April suggests that the relationship between atmospheric forcing and oceanic
response is not strictly simultaneous, and that the duration of the oceanic event may exceed that of the
wind anomaly that triggered it. The stronger and more sustained wind forcing in May 2025 (Fig. 7b) is
nonetheless consistent with the greater intensity and longer duration of the northward oceanic flow
observed relative to other events in the record (Figs. 2a,b), suggesting that whilst a sustained wind
540 anomaly is not required to maintain the flow indefinitely, its persistence is the primary control on the
overall duration and magnitude of the oceanic response.

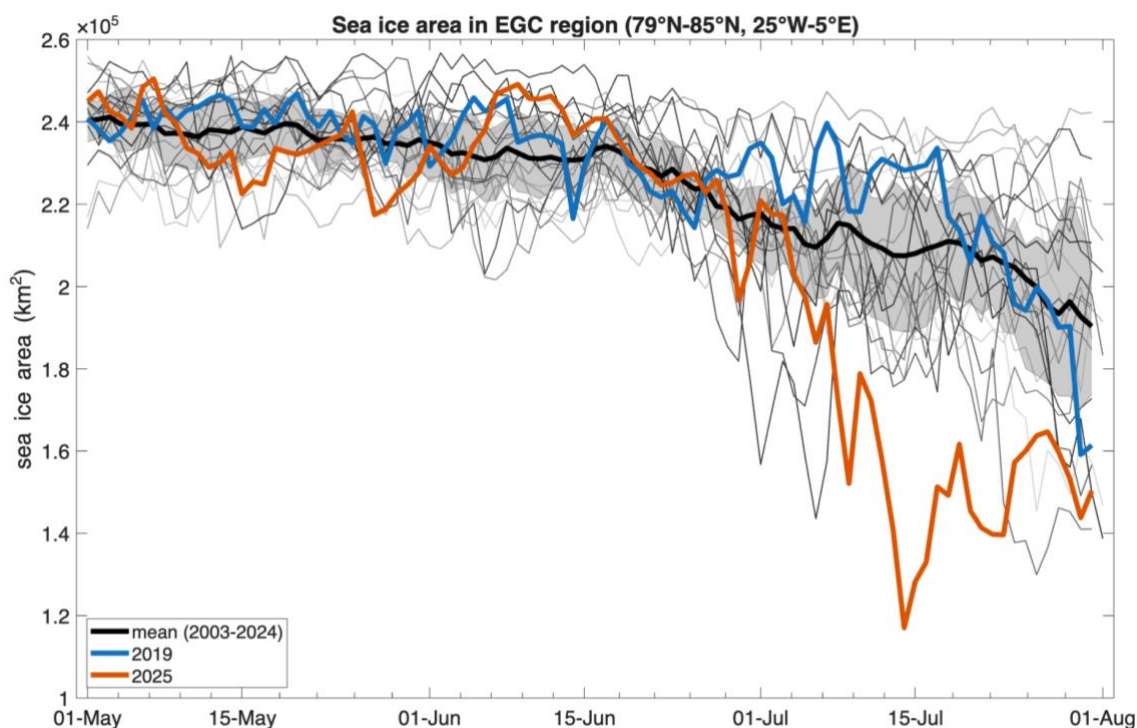
4.3. Northwards flow events and sea ice variability

The major 2025 northward flow event coincided with a period of exceptional sea ice loss on the
northeast Greenland continental shelf. Sea ice area averaged over the shelf tracked closely with the
545 2003-2024 mean through May and into mid-June, remaining within the interquartile range of the
historical record (Fig. 8). However, the area dropped sharply below the entire two-decade range by
early July and reached a record minimum of $\sim 1.2 \times 10^5$ km² around mid-July - lower than any
individual year in the satellite record at that point in the season. The abruptness of this decrease,
occurring within days rather than weeks, suggests dynamic atmospheric forcing and wind-driven ice
550 export rather than a more gradual thermodynamic response. In contrast, the 2019 sea ice area remained
within the range of historical variability throughout the summer months, despite the occurrence of a
northward deep flow event during that year.

Two possible connections between the May 2025 northward flow event and the subsequent July sea ice
555 anomaly are now considered, though it should be noted that the available observations permit us to
identify only possible contributors rather than establish causes. The first connection considered is
oceanic: the northward advection of anomalously warm AW during the northward event transported
poleward at depth (Fig. 5), with the potential to gradually erode the cold halocline from below and
reduce the stratification between the AW and surface PW, and thus reduce the barrier to heat flux at the
560 base of the sea ice. Temperatures at 50m at the 79°N mooring site are consistent with a modest oceanic
warming signal, increasing steadily from -1.7°C in early May to -1.5°C by mid-June 2025 which is
slightly elevated compared to the climatological mean at this depth for May (Fig. A2). Whilst this
anomaly is partly consistent with the expected seasonal warming, it may also reflect the upwelling
associated with the offshore displacement of the EGC core which would bring warmer subsurface water
565 to shallower depths (Fig. 9). Crucially, the 79°N mooring was recovered in mid-June 2025, and the



570 shallowest instrument at 50m lies below the surface mixed layer, precluding direct observation of near-surface ocean heat content during the period of peak sea ice area anomaly in July 2025. Whether the subsurface oceanic warming signal associated with the AW intrusion eroded the halocline sufficiently to influence upper ocean heat content on timescales relevant to sea ice loss therefore remains an open question that would require shallower observations to resolve. However, the abrupt drop in SIC during July is inconsistent with a primarily thermodynamic mechanism of driving ice loss which would produce a more gradual decline.



575 **Figure 8. Comparison of daily sea ice area north of the 79° mooring averaged over the region 79°N - 85°N, 25°W - 5°E in northeast Greenland between 1 May and 1 August 2003 - 2025). The blue and red lines are 2019 and 2025, respectively, the mean is the thick black line, and the interquartile range is the grey shaded area.**

580 The second, and likely more direct pathway, is atmospheric. The sustained northward winds associated with the northward flow events (Fig. 7c) would simultaneously have acted on the sea ice directly. Daily sea ice drift data provides independent evidence of this atmospheric forcing on the ice pack. At the onset of the 2025 event, the sea ice drift across Fram Strait and the East Greenland margin showed a pronounced but short-lived reversal from its typical southward state to anomalous northward drift that extended into the central Arctic (Fig. A6a), consistent with the anomalous northward wind forcing identified in May 2025 (Fig. 7b). This northward ice drift reversal persisted for approximately five days before the ice returned to its typical southward drift pattern (Fig. A6b), likely because the continuous upstream advection of ice from the Arctic interior overwhelmed the locally wind-driven northward signal. With a northward drift speed of ~15 km/day, this equates to a total northward sea ice drift of approximately 75 km. In contrast, the subsurface oceanic northward flow at 79°N persisted for at least



35 days with an upper bound of advection reach of 750 km — an order of magnitude longer and further
590 than the ice drift anomaly (Fig. 3b, 5b).

As the sea ice area in 2019 was not anomalously low (Fig. 8), a consistent link between northward flow
events and sea ice variability cannot be established from the current observations alone. The differences
in duration and intensity of northward velocities between the 2019 and 2025 events (Fig. 3a,b) however,
595 suggest that a threshold of forcing may need to be exceeded before a measurable sea ice response
emerges - one which was not reached in 2019. In practical terms, this threshold likely reflects both the
duration of anomalous northward wind forcing, which drives dynamic ice export, and the sustained
northward advection of warm AW at depth, which may gradually erode the halocline over weeks. The
2025 event, being nearly twice as strong and at least 20% longer than the 2019 event, and coinciding
600 with a period of record low sea-ice area in the region (Fig. 8) that may have made the ice pack more
susceptible to the same magnitude of forcing, appears to have exceeded this threshold where 2019 did
not. It is also noteworthy that the July 2004 sea ice area was also among the lowest values in the record,
coinciding with the strong 2004 northward flow event identified in the FSAOO mooring record at
78°50'N (Fig. A4). This co-occurrence of the exceptional SIC anomalies with the strongest northward
605 flow events suggests that such events, when sufficiently sustained and intense, can influence regional
sea ice variability. The northward transport of anomalously warm AW into the Arctic during events has
broader implications for the Arctic heat budget, since even episodic intrusions of warm Atlantic-origin
water at depth could contribute to the cumulative ocean heat available to delay ice formation or enhance
basal melt on seasonal timescales.

610 **5 Discussion**

The prolonged deep northward flow events documented in this study contribute a novel addition to the
conventional picture of the EGC as a persistent, year-round southward boundary current. Every
schematic circulation diagram of the Nordic Seas and Fram Strait depicts the EGC as a continuous
conduit for the export of cold, fresh Polar Water and Atlantic-origin water from the Arctic Ocean and
615 Fram Strait into the North Atlantic (e.g., Fig. 1) — a fundamental component of the large-scale Arctic
estuarine circulation. Whilst short-lived local northward flow events are not unexpected due to eddy
activity in Fram Strait (von Appen et al., 2016; Wekerle et al., 2020), the prolonged deep-reaching
northward flow events of 2019 and particularly 2025 are demonstrably outside the range of realistic
eddy dynamics in this region. These northward events therefore represent very different dynamics of the
620 boundary current system than previously been described at this location.

5.1 Proposed forcing mechanism

Building on the atmospheric observations in Section 4.2, it is proposed that deep northward flow events
are driven by anomalous northward wind along the East Greenland continental margin, which then
reorganises the boundary current system through two complementary oceanic responses.

625



First, an anomalous Ekman transport is set up toward the east, directed offshore, tending to displace the EGC core away from its climatological position over the shelf-break. Consistent with this, the shipboard velocity (VMADCP) section at 79°N during the 2025 event shows that the EGC, typically southward as observed at 5°23.8'W over the ~1000m isobath (Fig. A1), was observed offshore, at 4°45'W over the 1400m isobath (Fig. 2c). In May 2019, the baroclinic velocity core at about 750-1000 m of the shelfbreak EGC at 78° 50'N, which normally resides around 4°W (Fig. 6b), shifted to approximately 3°W and maximum surface velocities were seen as far east as 2°W with an anomaly of almost 0.1 ms⁻¹ (Fig. 6d).

Second, and more directly relevant to the northward flow itself, sustained northward winds imposing a northward along-slope wind stress to the boundary current over periods of weeks can drive a lateral reorganisation of the EGC system. The northward wind anomaly generates cross-slope eastward Ekman transport that diverges near the coast, reducing sea surface height and setting up barotropic pressure gradients that displace the southward flowing EGC core offshore, away from its climatological position over the shelf-break (maintained by climatological northerly winds) (Fig. 9), while wind-driven and geostrophically adjusted flow on the inner slope and shelf can weaken the EGC core and produce a net northward current inshore of the shelf-break boundary current, given that the flow there was already weak (Fig. 6b). This is demonstrated by the change in velocity structure with northward velocities on the shelf break and reduced southwards velocities offshore (Fig. 6d). This adjustment occurs over timescales of hours to days - on the order of the inertial period at 79°N (~12 hours) for the initial Ekman response - extending to weeks as the full barotropic geostrophic adjustment of the boundary current system responds to the sustained forcing.

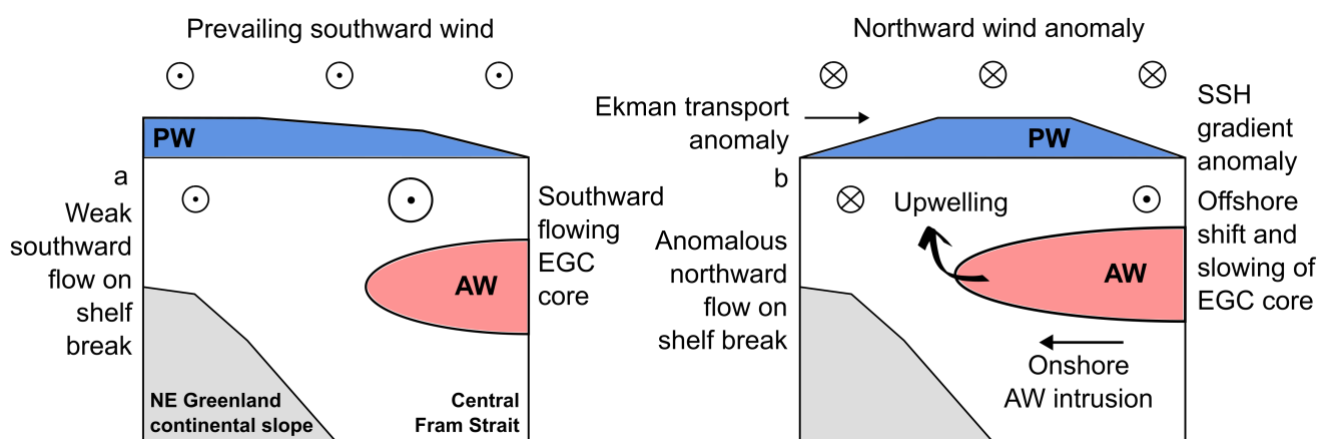


Figure 9. Schematic cross-section of the Northeast Greenland continental shelf and central Fram Strait illustrating (a) the mean state with Polar Water (PW) surface layer, and Atlantic Water (AW) at depth, and (b) the reorganisation of the boundary current system under anomalous wind forcing. The northward wind anomaly drives eastward Ekman transport that generates a positive sea surface height (SSH) gradient and displaces the EGC core offshore. Compensating upwelling over the continental slope raises warm AW to shallower depths, while the along-slope wind forcing and geostrophically adjusted flow produces northward flow at the shelf break.

The lateral reorganization of the EGC current system, as e.g. seen in 2019 (Fig. 6), is broadly consistent with wind-driven adjustment of a boundary current system. In particular, sustained northward wind anomalies and more particularly associated anomalies in the wind stress curl could plausibly modify the prevailing onshore Ekman flow and regions of convergence/divergence of the Ekman transport. In turn, this would be expected to modify sea surface height gradients and the barotropic pressure field across the shelf break maintaining the EGC. Such adjustments may provide a pathway for lateral displacement of the EGC core away from the shelf break and dynamical explanation for the northward flow events, consistent with the mooring observations.

The exceptional duration of the 2025 event relative to other deep events in the mooring record (Fig 3b) therefore likely reflects the anomalous persistence of the northward wind anomaly during those events, rather than a fundamentally different forcing mechanism. An atmospheric forcing mechanism is supported by the behaviour of the hydrographic structure during the northward events. Whilst the T-S properties and vertical stratification at the 79°N mooring site were anomalous during both 2019 and 2025 events (Fig. 4), reflecting the subsurface intrusion of Atlantic-origin waters from the WSC, the cross-slope density gradient that sets the background geostrophic structure of the EGC remained intact, observed by the persistence of isopycnals consistent with southward geostrophic flow below 500m (Fig 2). The anomalous water mass properties at depth are therefore interpreted as a consequence of the wind-forced shift of the boundary current rather than its cause. The sustained northward wind advects warm AW from where there is stronger recirculation at 78°50'N than at 79°N (de Steur et al., 2014), and produces upwelling over the continental slope associated with the offshore Ekman transport which raises AW from its typical depth range to shallower levels (Fig. 9). Both can act to bring anomalously warm AW into contact with the mooring instruments at 250m, and likely operate simultaneously as part of the same wind-driven response. However, the single-point mooring observations cannot distinguish their relative contributions.

5.2 Sea ice response and ocean-ice interactions

The sea ice response to the 2025 flow event was predominantly dynamic rather than thermodynamic in character. The abrupt onset of the sea ice area anomaly in early July 2025 (Fig. 8), occurring approximately 6-8 weeks after the start of the northwards oceanic flow event and following the period of anomalous northward atmospheric forcing in May (Fig. 7b), is consistent with a lagged response to the combined oceanic and atmospheric forcing rather than a direct and immediate thermodynamic signal. The partial increase in sea ice area after mid-July is also consistent with dynamic forcing rather than thermodynamic melting, which would produce a smoother and more sustained decline. The role of persistent northward winds in driving large-scale sea ice variability along the northeast Greenland margin is well established. Detailed modelling and satellite analyses of major polynya events in this region conclude that strong, persistent northward winds drive mechanical export and deformation of the ice pack, with ocean heat playing a secondary rather than primary role in ice loss (Bennett et al., 2024; Lee et al., 2023). Ludwig and Krumpfen (2026) further note that sea ice in the Northeast Greenland region is predominantly dynamically driven and does not exhibit a statistically significant long-term trend, as the continuous resupply of ice from upstream typically maintains a closed ice cover. The

pronounced drop in July 2025 is therefore all the more striking and suggests a specific forcing event as the primary driver rather than gradual long-term decline. In turn, the resulting reduction in sea ice concentration increases the open water area available for solar radiation absorption, potentially warming the upper ocean and further inhibiting ice formation (de Steur et al., 2023).

700

The divergence in response timescales between the sea ice and the subsurface ocean - with the ice drift reversal lasting approximately five days (Fig. A6) whilst the oceanic northward flow persisted for at least 35 days (Fig 3b) - reflects different inertia of the two systems, and has further implications for upper ocean heat exchange. During this period of temporary vertical decoupling, the opposing motion between the southward-drifting sea ice and surface layer and the northward-flowing subsurface current may also generate enhanced vertical shear across the upper halocline. This shear-driven turbulence could facilitate upward entrainment of warm AW into the overlying cold halocline - a process operating on shorter timescales than gradual thermodynamic halocline erosion which may be more relevant to the rapid July sea ice anomaly (Fig. 8) given its shorter timescale.

710

The impact of these northward deep flow events on sea ice is further modulated by the seasonal state of the ice pack at the time of forcing. Sea ice drift speeds in the Arctic decrease markedly from around May onwards as the ice pack weakens and becomes more mobile (Olason and Notz, 2014), reducing the resistance of the ice to wind-driven deformation and export. This seasonal vulnerability may explain in part why the spring-dominated timing of northward flow events (Fig. 3c) coincides with a period when the ice pack is most susceptible to dynamic forcing. Furthermore, the long-term thinning and areal reduction of Arctic sea ice means that the same atmospheric forcing can now drive larger ice responses than in previous decades, as thinner ice is more easily deformed and exported (Sumata et al., 2023). Sumata et al., (2022) found that the anomalously reduced ice export in 2018 was attributed to regional sea ice-ocean processes driven by anomalous atmospheric circulation over the Atlantic sector of the Arctic - consistent with the forcing pattern identified here - suggesting that the atmospheric conditions associated with northward flow events may suppress southward ice export more broadly across the region. A positive feedback may therefore operate: northward flow events stall the southward export of sea ice whilst simultaneously advecting warm AW northward, reducing ice area and thickness and in turn making the system more susceptible to subsequent atmospheric forcing events.

715

720

725

5.3 Broader implications for Arctic heat pathways

Beyond the regional sea ice response, the northward flow events documented here have broader implications for ocean heat transport into the Arctic interior. A direct consequence of these northward flow events is the establishment of an episodic northward pathway for warm Atlantic-origin water into a region otherwise dominated by the southward export of cold and fresh Arctic water masses. During both the 2019 and 2025 events, anomalously warm AW - with T-S properties very similar to the WSC recirculation across Fram Strait (Fig. 4) - was advected northward at depth. If the northward flow had been sustained at the observed velocity throughout each event's duration, AW would have reached estimated horizontal displacements of approximately 250 km during the 2019 event and up to 750 km

730



735 during the 2025 event (Fig. 5). These are the latitudes where Atlantic heat has been increasingly
implicated in sea ice loss and upper ocean warming through Atlantification (Polyakov et al., 2017).

While these are upper-bound estimates, even a fraction of this displacement represents a significant
injection of Atlantic heat into a part of the Arctic that is not typically exposed to the direct influence of
740 AW. The AW transported northward during these events is warmer than the AAW that is typically
found subsurface in the EGC (Fig 4), and its northward advection at depth — insulated from the surface
by the cold fresh PSW layer (Fig 2) — means that this heat enters the Arctic interior where it may
contribute to the subsurface ocean heat reservoir rather than being immediately lost to the atmosphere or
745 sea ice. The co-occurrence of the 2025 event with the record low July sea ice area in the EGC region
(Fig. 8), is consistent with the idea that these events have tangible consequences for the regional sea ice
state, though establishing a direct and quantitative causal link remains an important objective for future
work. The cumulative effect of repeated northward flow events, even if episodic, could therefore
represent an additional, non-negligible contribution to the Arctic heat budget through a previously
750 unrecognised pathway through which Atlantic heat can penetrate the Arctic, complementing the better-
documented inflow through the Barents Sea opening and the WSC (Ingvaldsen et al., 2004; Skagseth et
al., 2008; McPherson et al., 2026).

The occurrence of a similarly large anomalous northward flow of the shelfbreak EGC north of Denmark
Strait, attributed to a large anticyclonic event and described by de Steur et al., (2017), suggests that
755 prolonged northward flow along the east Greenland continental slope may be a more widespread feature
of the system than has been reported. This raises a question: are these anomalous events rare but
intrinsic features of a naturally variable boundary current system, or do they represent an early signal of
ongoing change in the Arctic-Atlantic exchange? The identification of 8 deep-reaching northward flow
events over the extended record at 78°50'N between 2003 and 2019 further demonstrates that episodic
760 northward flow at the East Greenland shelf-break is not unique to the recent observations at 79°N. At
the same time, the exceptional duration of the 2025 event — the longest resolved in either dataset —
and its co-occurrence with record low sea ice area suggests that whilst the phenomenon itself is not
new, its most extreme expressions may be becoming more frequent or intense as Arctic conditions
continue to change. It is also possible that the changing Arctic — characterised by warming Atlantic
765 waters (McPherson et al., 2026; Polyakov et al., 2023), declining sea ice (Krumpfen et al., 2025; Sumata
et al., 2023), and modified density gradients across Fram Strait (Karam et al., 2024; Karpouzoglou et
al., 2024, 2022) — is creating conditions increasingly favourable for sustained northward intrusions of
AW into the EGC. Longer observational records, increased measurements along the East Greenland
margin, and targeted modelling studies would be needed to distinguish between these possibilities and
770 to quantify the contribution of episodic northward flow events to Arctic heat and freshwater budgets.

Finally, a potentially related signal can be observed in the freshwater transport record. Southward
freshwater transport across the NPI array at 78°50'N in summer 2019 was at its lowest since 2003, part
of a longer-term reduced freshwater export between 2016 and 2019 attributed to reduced EGC volume
775 transport and salinification of the lower halocline (Karpouzoglou et al., 2022). Whilst a direct link to the
northward flow events documented here is difficult to establish, the reduced southward velocity of the

EGC during this period is dynamically consistent with the atmospheric forcing patterns identified in Section 4.1.2, suggesting that the observed events may represent the most extreme expression of a more persistent weakening of the EGC boundary current during this period. Whether the northward events documented here contributed to, or were symptomatic of, this broader freshwater transport decline remains an open question that warrants further investigation with a longer observational record.

6 Conclusions

The East Greenland Current (EGC) is the main conveyor of cold and fresh Polar Water and sea ice from the Arctic Ocean to the subpolar North Atlantic. Long-term mooring observations (2018 - 2025) on the East Greenland continental slope at 79°N reveal that whilst the EGC maintains a persistent southward flow throughout the year, it is punctuated by periodic northward flow events, spanning a wide range of durations and vertical coherence. The majority of these events are short-lived (fewer than 5 days) local northward flow events, consistent with eddy timescales and energy levels characteristic of the western Fram Strait. However, two prolonged deep-reaching events — in April–May 2019 (29 days) and May–June 2025 (at least 35 days) — stand out as anomalous in their duration, strength and vertical coherence (down to at least 500 m), with mean northward velocities exceeding the climatological May mean by 1.7 and 2.7 standard deviations for the 2019 and 2025 events respectively. The velocity magnitude of the 2025 event was almost double that of 2019, representing an unprecedented occurrence in the historical mooring record at this location. During both events, hydrographic observations revealed anomalous dominance of warm Atlantic-origin water at depths typically occupied by cooler Arctic Atlantic Water, weakened vertical stratification, and T-S properties consistent with recent derivation from the West Spitsbergen Current recirculation across Fram Strait. The extended FSAOO mooring array record at 78°50'N (2003 - 2019) also identified the 2019 event, revealing that while the northward flow signal was spatially confined to the continental shelf-break, comparison of the long-term May mean and the May 2019 velocity section (during which the 2019 event occurred) showed a coherent weakening of southward flow and offshore displacement of the EGC core extending across the continental slope to at least the 2500m isobath. This identifies these events as regional rather than purely locally driven. The FSAOO record at 78°50'N further showed a total of 8 deep-reaching northward flow events, including two particularly strong events in 2004 and 2008. This demonstrates that episodic northward flow at the East Greenland shelf-break is an intrinsic and recurring feature of the EGC system rather than a phenomenon unique to the recent observational period.

The characteristics of the two prolonged deep northward flow events in 2019 and 2025 are inconsistent with eddy-driven forcing on geometric and energetic grounds, ruling out mesoscale eddies as their primary driver. Atmospheric reanalysis reveals a persistent SLP dipole with anomalous northward winds along the East Greenland margin and through Fram Strait during both 2019 and 2025 events, and a composite of all anomalously strong deep northward flow events shows a broadly similar wind forcing pattern, suggesting that anomalous northward winds are a recurring feature of these events.



815 It is proposed here that the sustained northward wind anomaly drives a lateral reorganisation of the
boundary current system. A cross-slope eastward Ekman transport that diverges near the coast reduces
the sea surface height and sets up a barotropic pressure gradient that displaces the EGC core offshore
and away from its climatological position over the shelf-break. The wind-driven and geostrophically
adjusted flow on the inner slope produces a net northward current inshore where the flow was already
820 weak, without implying a wholesale reversal of the EGC itself. The anomalously warm AW observed at
depth during both events is interpreted as a consequence of this wind-forced reorganisation, arising
through two complementary pathways: the northward advection of recirculating AW from further south
along the shelf-break, and upwelling over the continental slope associated with the offshore Ekman
displacement. The atmospheric forcing in May 2019 had already weakened relative to April 2019, when
825 the 2019 event began, though the northward oceanic flow persisted, indicating that the boundary current
system retains its geostrophic adjustment beyond the period of active wind forcing, reflecting the inertia
of the adjustment process rather than a direct and immediate response to wind stress.

The co-occurrence of the 2025 event with record low July sea ice area in the northeast Greenland region
830 is consistent with tangible regional consequences for sea ice. The abrupt onset, and partial recovery, of
the sea ice anomaly point toward dynamic atmospheric forcing and wind-driven ice export as the
primary driver rather than thermodynamic basal melting, which would produce a more gradual and
sustained decline. No significant sea ice anomaly in 2019 suggests a threshold of combined forcing
duration and strength must be exceeded before there is a detectable sea ice response. More broadly, a
835 direct consequence of these northward flow events is the establishment of an episodic northward
pathway for warm Atlantic Water into a region otherwise dominated by Arctic outflow — a previously
unrecognised mode of Atlantic heat transport into the Arctic interior, with potential reach of hundreds
of kilometres beyond the mooring location. Given the much thinner and reduced sea ice coverage,
especially in summer, these events may occur more frequently nowadays, allowing for a more direct
840 coupling (or impact) of atmospheric variations with ocean dynamics.

Whether the prolonged northward flow events documented here represent rare but intrinsic features of a
naturally variable boundary current system, or early signals of ongoing change in the Arctic-Atlantic
exchange, cannot be determined from the current observational record alone. Resolving this question,
845 and quantifying the contribution of episodic northward flow to Arctic heat, freshwater and sea-ice
budgets, would require longer observational records along the East Greenland margin, targeted
idealized modelling studies, and a more complete atmospheric reconstruction spanning the onset and
duration of individual northward flow events. A first step will come with the planned recovery of the
current EGC mooring at 79°N in summer 2026, which will resolve the full duration of the 2025 event
850 and capture any subsequent northward flow events, providing a critical extension of the observational
record at this key location.



Appendix A

Depth (m)	Instrument	Variable Sampled	Sampling Rate
54	SBE37-SMP-ODO (Sea-Bird Scientific)	T/S	10 minutes
61	SeaGuard RCM (Aanderaa)	u/v	1 hour
230	SBE37-SMP-ODO (Sea-Bird Scientific)	T/S	10 minutes
233	RCM11 (Aanderaa)	u/v	1 hour
494	SBE37-SMP-ODO (Sea-Bird Scientific)	T/S	10 minutes
496	RCM11 (Aanderaa)	u/v	1 hour

Table A1. Configuration of the 79°N mooring in the EGC (17 July 2024 - 22 June 2025). This is typical of the mooring layout since 2018. Variables are T (temperature), S (salinity), and u/v (zonal/ meridional components of velocity).

855

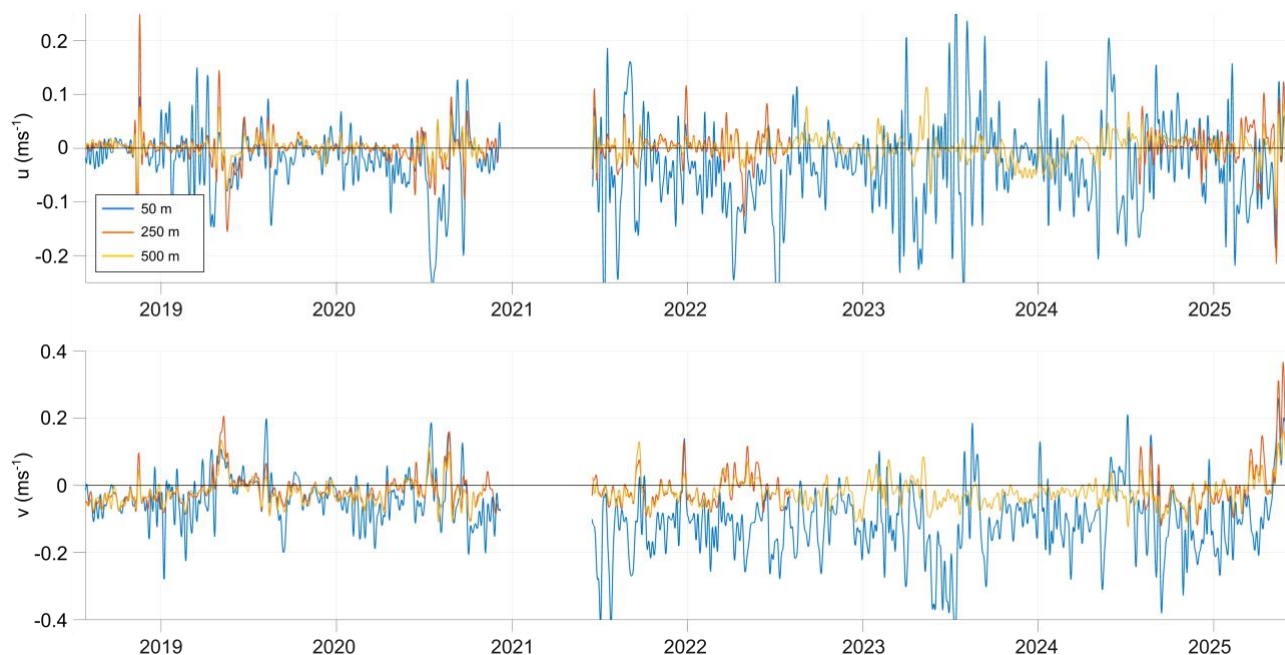
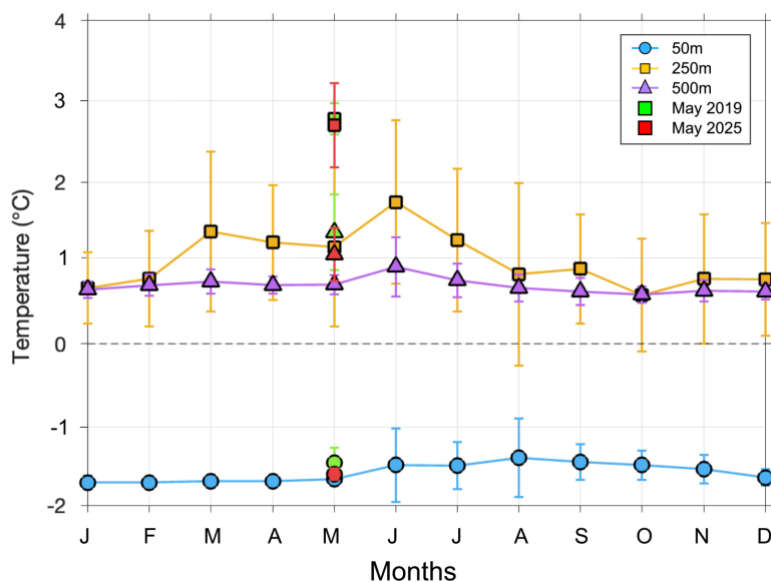
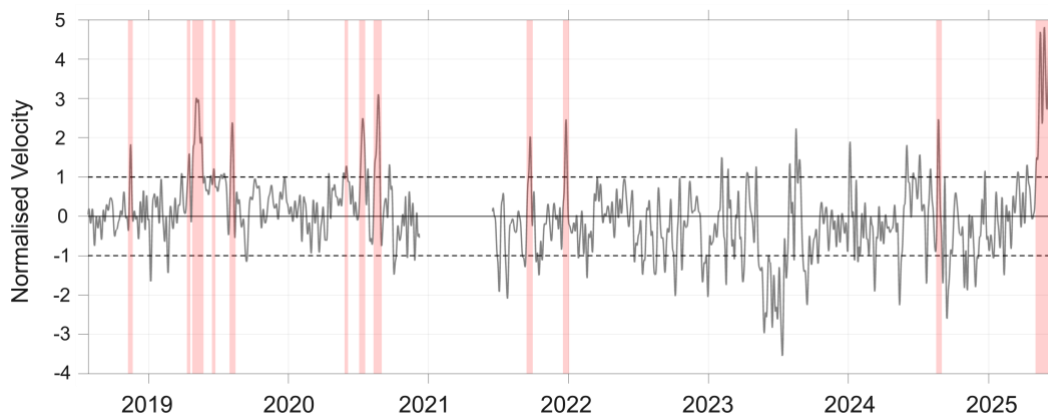


Figure A1. Time series of (a) zonal (u) and (b) meridional (v) velocities from the 79°N mooring at nominal depths of 50m (blue), 250m (orange), 500m (yellow) between July 2018 - June 2025.



860 **Figure A2.** Seasonal cycle of potential temperature at 50 m (blue), 250m (orange), and 500 m (purple) at the 79°N mooring between 2018 - 2025. The mean temperatures in May 2019 and May 2025 at each of the three depths are marked by the green and red symbols (circle = 50m; square = 250m; triangle = 500m) respectively. Whiskers represent the standard deviation.



865 **Figure A3.** Time series of normalised velocities averaged over the upper 500m at the 79°N EGC mooring location with the deep northwards events in red. The dashed lines indicated velocities that are one standard deviation above and below the mean. Note that not all anomalously strong northwards flows were deep-reaching.

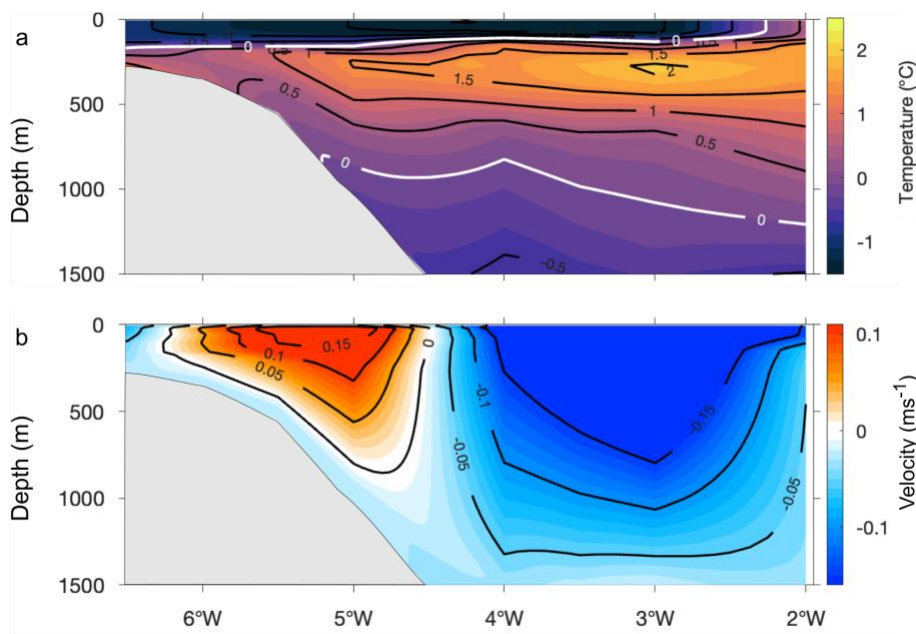
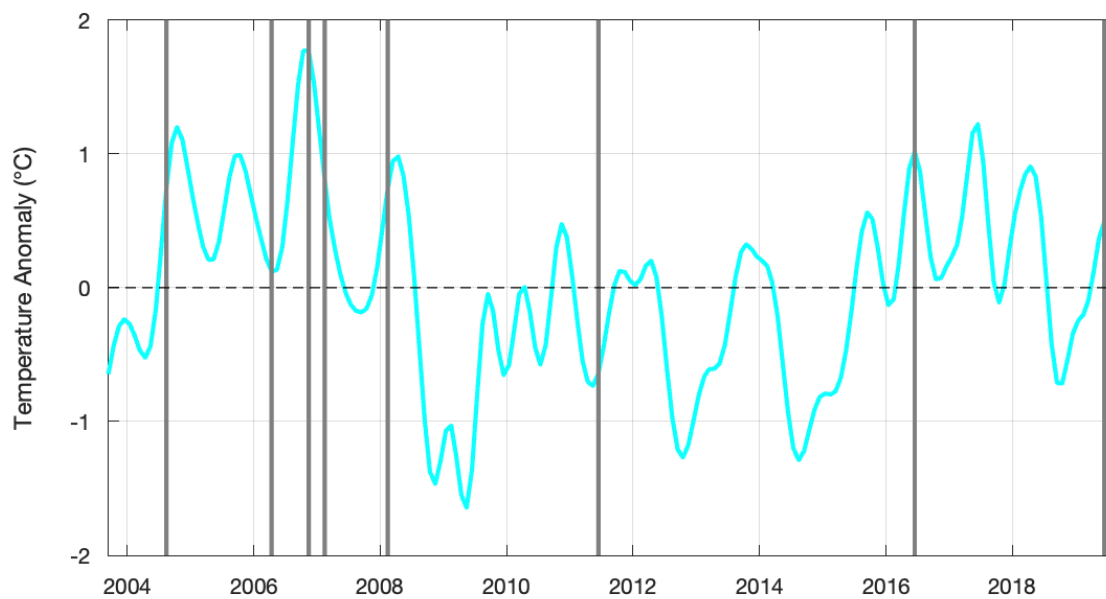
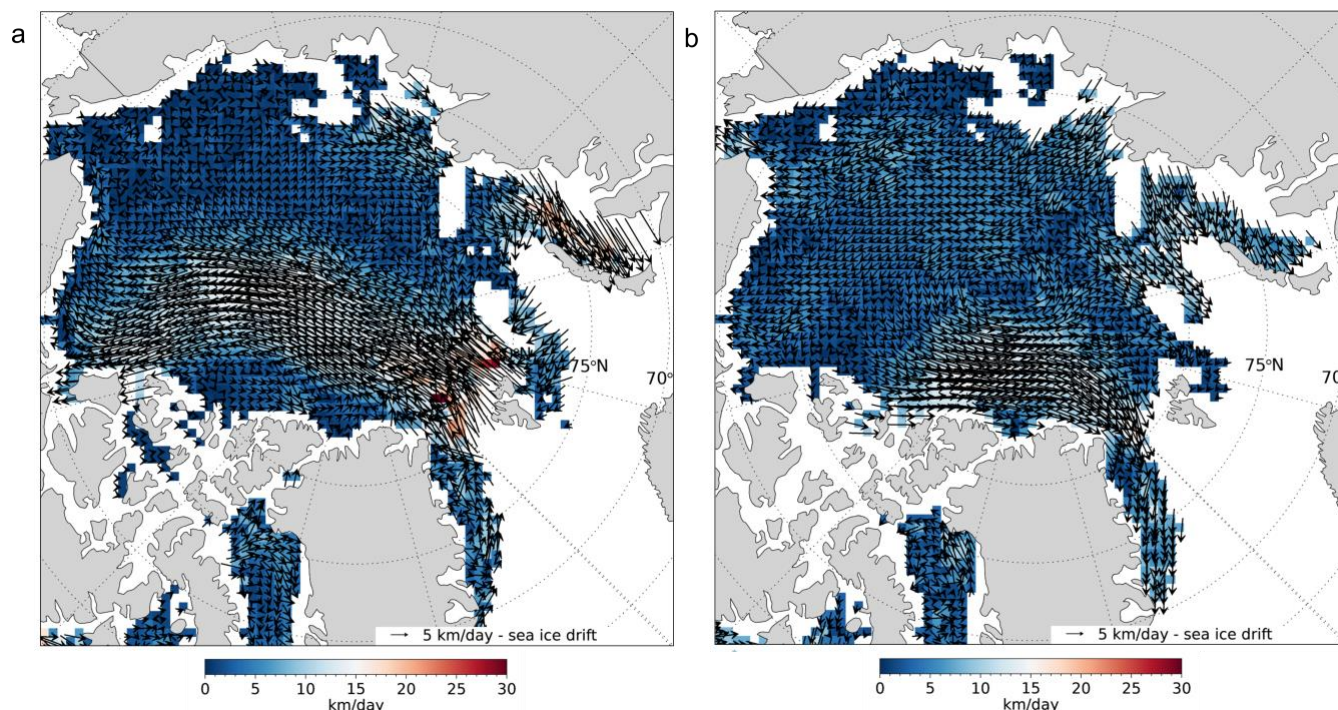


Figure A4. Average sections of (a) potential temperature and (b) northward velocity in June 2004 across the FSAOO mooring array at 78°50'N.



870

Figure A5. Time series of climatological temperature anomaly of the AW at 250m between 5°W - 5° 45'W at the FSAOO mooring array. The vertical lines are the timing of the deep-reaching northward flow events identified at this location.



875 **Figure A6.** Map of daily sea ice drift velocity (color) and direction (arrows) (a) during the short-lived anomalous northward drift (07 May 2025) and (b) representative of the typical southward drift state following the return to background conditions (18 May 2025).

Data availability

880 Hydrographic and velocity data from the 79°N mooring from 2018 - 2022 is accessible from Hoppmann (2026). CTD and LADCP data from summer 2025 (PS148) will soon be available (data upload in progress). The FSAOO mooring gridded data set at 78° 50'N from 2003 - 2019 is available from Karpouzoglou et al., (2021). Atmospheric reanalysis is ERA5 monthly averaged data on pressure levels from 1940 to present, from the Copernicus Climate Change Service (C3S) Climate Data Store (CDS) (Copernicus Climate Change Service, 2019). Daily mean sea ice area data since 2003 can be obtained from the University of Bremen (www.seaice.uni-bremen.de). Sea ice motion data were obtained from the Ocean and Sea Ice Satellite Application Facility (OSI SAF) at <https://osi-saf.eumetsat.int>.
885

Author contributions

890 RM conducted the experiment, analysed the oceanography data and prepared the manuscript. WJvA designed the experiment, acquired funding, and supervised. LdS contributed data and aided in the interpretation and overall direction of the manuscript. LB analysed data. MI, TK, and GS contributed data and interpretation. FOH analysed data and contributed to its visualisation. All co-authors contributed to the writing of the manuscript and their respective data interpretation.



Competing interests

The authors declare that they have no conflict of interest

895 Disclaimer

Copernicus Publications remains neutral with regard to jurisdictional claims made in the text, published maps, institutional affiliations, or any other geographical representation in this paper. While Copernicus Publications makes every effort to include appropriate place names, the final responsibility lies with the authors. Views expressed in the text are those of the authors and do not necessarily reflect the views of
900 the publisher.

Acknowledgements

This work is funded by the European Union as part of the EPOC project (Explaining and Predicting the Ocean Conveyor). Views and opinions expressed are however those of the author(s) only and do not necessarily reflect those of the European Union. Neither the European Union nor the granting authority
905 can be held responsible for them. This work is also funded by the Agencia Estatal de Investigación AEI-DFG project MIXSED (“Mixing and Sediment Dynamics”) funded by the through the PCI 2024 call – project PCI2024-155022-2 and PCI2024-155084-2 and the Deutsche Forschungsgemeinschaft (DFG, German Research Foundation) – Projektnummer 541914507. GS acknowledges funding by the
910 Deutsche Forschungsgemeinschaft (DFG) through the SFB/TRR 172 (AC)³ – Arctic Amplification (Project-ID 268020496). We would also like to acknowledge the long-term observations from the Fram Strait Arctic Outflow Observatory (FSAOO) at 78°50’N in the western Fram Strait which has been made possible by the Norwegian Polar Institute. We acknowledge the help of Dr. Janna Rückert, University of Bremen in pre-processing the sea ice concentration data.

915 We thank the captains, crews, and scientific parties on the R/V Polarstern during the multiple expeditions, and specifically to Normen Lochthofen and Lutz Peine for first identifying this phenomenon in the field. Thanks also to all who processed the Fram Strait mooring data over the years. The following cruises (listed with grant numbers) contributed to the maintenance of the EGC 79°N mooring: PS114 (AWI_PS114_01), PS121 (AWI_PS121_06), PS126 (AWI_PS126_07), PS131
920 (AWI_PS131_04), PS136 (AWI_PS136_04), PS143.2 (AWI_PS143.2_00); PS148 (AWI_PS148_02).



References

- Aagaard, K., Coachman, L.K., 1968a. The East Greenland Current North of Denmark Strait: Part I. ARCTIC 21, 181–200. <https://doi.org/10.14430/arctic3262>
- Aagaard, K., Coachman, L.K., 1968b. The East Greenland Current North of Denmark Strait: Part II. ARCTIC 21, 267–290. <https://doi.org/10.14430/arctic3270>
- Aagaard, K., Foldvik, A., Hillman, S.R., 1987. The West Spitsbergen Current: Disposition and water mass transformation. *J. Geophys. Res.* 92, 3778. <https://doi.org/10.1029/JC092iC04p03778>
- 930 Bashmachnikov, I.L., Kozlov, I.E., Petrenko, L.A., Glok, N.I., Wekerle, C., 2020. Eddies in the North Greenland Sea and Fram Strait From Satellite Altimetry, SAR and High-Resolution Model Data. *J. Geophys. Res. Oceans* 125, e2019JC015832. <https://doi.org/10.1029/2019JC015832>
- Bennett, M.G., Renfrew, I.A., Stevens, D.P., Moore, G.W.K., 2024. The Northeast Water Polynya, Greenland: Climatology, Atmospheric Forcing and Ocean Response. *J. Geophys. Res. Oceans* 129, e2023JC020513. <https://doi.org/10.1029/2023JC020513>
- 935 Copernicus Climate Change Service, 2019. ERA5 monthly averaged data on pressure levels from 1940 to present. <https://doi.org/10.24381/CDS.6860A573>
- Dannheim, J., 2025. The Expedition PS148 of the Research Vessel POLARSTERN to the Arctic Ocean in 2025. Alfred-Wegener-Institut Helmholtz-Zentrum für Polar- und Meeresforschung. https://doi.org/10.57738/BZPM_0803_2025
- 940 de Steur, L., Hansen, E., Mauritzen, C., Beszczynska-Möller, A., Fahrbach, E., 2014. Impact of recirculation on the East Greenland Current in Fram Strait: Results from moored current meter measurements between 1997 and 2009. *Deep Sea Res. Part Oceanogr. Res. Pap.* 92, 26–40. <https://doi.org/10.1016/j.dsr.2014.05.018>
- 945 de Steur, L., Peralta-Ferriz, C., Pavlova, O., 2018. Freshwater Export in the East Greenland Current Freshens the North Atlantic. *Geophys. Res. Lett.* 45, 13,359–13,366. <https://doi.org/10.1029/2018GL080207>
- de Steur, L., Pickart, R.S., Macrander, A., Våge, K., Harden, B., Jónsson, S., Østerhus, S., Valdimarsson, H., 2017. Liquid freshwater transport estimates from the East Greenland Current based on continuous measurements north of Denmark Strait. *J. Geophys. Res. Oceans* 122, 93–109. <https://doi.org/10.1002/2016JC012106>
- 950 de Steur, L., Sumata, H., Divine, D.V., Granskog, M.A., Pavlova, O., 2023. Upper ocean warming and sea ice reduction in the East Greenland Current from 2003 to 2019. *Commun. Earth Environ.* 4, 261. <https://doi.org/10.1038/s43247-023-00913-3>
- 955 Haine, T.W.N., Curry, B., Gerdes, R., Hansen, E., Karcher, M., Lee, C., Rudels, B., Spreen, G., De Steur, L., Stewart, K.D., Woodgate, R., 2015. Arctic freshwater export: Status, mechanisms, and prospects. *Glob. Planet. Change* 125, 13–35. <https://doi.org/10.1016/j.gloplacha.2014.11.013>



- Hattermann, T., Isachsen, P.E., Appen, W., Albretsen, J., Sundfjord, A., 2016. Eddy-driven recirculation of Atlantic Water in Fram Strait. *Geophys. Res. Lett.* 43, 3406–3414.
960 <https://doi.org/10.1002/2016GL068323>
- Håvik, L., Pickart, R.S., Våge, K., Torres, D., Thurnherr, A.M., Beszczynska-Möller, A., Walczowski, W., von Appen, W.-J., 2017. Evolution of the East Greenland Current from Fram Strait to Denmark Strait: Synoptic measurements from summer 2012. *J. Geophys. Res. Oceans* 122, 1974–1994.
<https://doi.org/10.1002/2016JC012228>
- 965 Håvik, L., Våge, K., 2018. Wind-Driven Coastal Upwelling and Downwelling in the Shelfbreak East Greenland Current. *J. Geophys. Res. Oceans* 123, 6106–6115. <https://doi.org/10.1029/2018JC014273>
- Hersbach, H., Bell, B., Berrisford, P., Hirahara, S., Horányi, A., Muñoz-Sabater, J., Nicolas, J., Peubey, C., Radu, R., Schepers, D., Simmons, A., Soci, C., Abdalla, S., Abellan, X., Balsamo, G., Bechtold, P., Biavati, G., Bidlot, J., Bonavita, M., De Chiara, G., Dahlgren, P., Dee, D., Diamantakis, M., Dragani, R., Flemming, J., Forbes, R., Fuentes, M., Geer, A., Haimberger, L., Healy, S., Hogan, R.J., Hólm, E., Janisková, M., Keeley, S., Laloyaux, P., Lopez, P., Lupu, C., Radnoti, G., De Rosnay, P., Rozum, I., Vamborg, F., Villaume, S., Thépaut, J., 2020. The ERA5 global reanalysis. *Q. J. R. Meteorol. Soc.* 146, 1999–2049. <https://doi.org/10.1002/qj.3803>
- 970 Hofmann, Z., von Appen, W., Wekerle, C., 2021. Seasonal and Mesoscale Variability of the Two Atlantic Water Recirculation Pathways in Fram Strait. *J. Geophys. Res. Oceans* 126, 1–18.
<https://doi.org/10.1029/2020JC017057>
- Hoppmann, M., 2026. Collection of raw data from oceanographic moorings in the Fram Strait, Greenland Sea, and central Arctic Ocean, 2018–2025. <https://doi.org/10.1594/PANGAEA.959812>
- 975 Ingvaldsen, R.B., Asplin, L., Loeng, H., 2004. The seasonal cycle in the Atlantic transport to the Barents Sea during the years 1997–2001. *Cont. Shelf Res.* 24, 1015–1032.
<https://doi.org/10.1016/j.csr.2004.02.011>
- Ionita, M., Scholz, P., Lohmann, G., Dima, M., Prange, M., 2016. Linkages between atmospheric blocking, sea ice export through Fram Strait and the Atlantic Meridional Overturning Circulation. *Sci. Rep.* 6, 32881. <https://doi.org/10.1038/srep32881>
- 985 Isachsen, P.E., LaCasce, J.H., Mauritzen, C., Häkkinen, S., 2003. Wind-Driven Variability of the Large-Scale Recirculating Flow in the Nordic Seas and Arctic Ocean. *J. Phys. Oceanogr.* 33, 2534–2550.
[https://doi.org/10.1175/1520-0485\(2003\)033%3C2534:WVOTLR%3E2.0.CO;2](https://doi.org/10.1175/1520-0485(2003)033%3C2534:WVOTLR%3E2.0.CO;2)
- Jónsson, S., Foldvik, A., Aagaard, K., 1992. The structure and atmospheric forcing of the mesoscale velocity field in Fram Strait. *J. Geophys. Res. Oceans* 97, 12585–12600.
990 <https://doi.org/10.1029/92JC01195>
- Karam, S., Heuzé, C., Hoppmann, M., De Steur, L., 2024. Continued warming of deep waters in the Fram Strait. *Ocean Sci.* 20, 917–930. <https://doi.org/10.5194/os-20-917-2024>
- Karpouzoglou, T., de Steur, L., 2021. Fram Strait gridded monthly mean velocity and salinity and time-series of freshwater transport, freshwater content, volume transport and salt transport since 2003.
995 <https://doi.org/10.21334/NPOLAR.2021.049178D8>
- Karpouzoglou, T., De Steur, L., Smedsrud, L.H., Karcher, M., Sumata, H., 2024. Three Forcing Mechanisms of Freshwater Transport in Fram Strait. *J. Geophys. Res. Oceans* 129, e2024JC020930.
<https://doi.org/10.1029/2024JC020930>



- 1000 Karpouzoglou, T., de Steur, L., Smedsrud, L.H., Sumata, H., 2022. Observed Changes in the Arctic Freshwater Outflow in Fram Strait. *J. Geophys. Res. Oceans* 127, e2021JC018122. <https://doi.org/10.1029/2021JC018122>
- Krumpen, T., Von Albedyll, L., Bünger, H.J., Castellani, G., Hartmann, J., Helm, V., Hendricks, S., Hutter, N., Landy, J.C., Lisovski, S., Lüpkes, C., Rohde, J., Suhrhoff, M., Haas, C., 2025. Smoother sea ice with fewer pressure ridges in a more dynamic Arctic. *Nat. Clim. Change* 15, 66–72. <https://doi.org/10.1038/s41558-024-02199-5>
- 1005 Krumpen, T., Von Albedyll, L., Goessling, H.F., Hendricks, S., Juhls, B., Spreen, G., Willmes, S., Belter, H.J., Dethloff, K., Haas, C., Kaleschke, L., Katlein, C., Tian-Kunze, X., Ricker, R., Rostosky, P., Rückert, J., Singha, S., Sokolova, J., 2021. MOSAiC drift expedition from October 2019 to July 2020: sea ice conditions from space and comparison with previous years. *The Cryosphere* 15, 3897–3920. <https://doi.org/10.5194/tc-15-3897-2021>
- 1010 Le Bras, I., Straneo, F., Muilwijk, M., Smedsrud, L.H., Li, F., Lozier, M.S., Holliday, N.P., 2021. How Much Arctic Fresh Water Participates in the Subpolar Overturning Circulation? *J. Phys. Oceanogr.* 51, 955–973. <https://doi.org/10.1175/jpo-d-20-0240.1>
- 1015 Le Bras, I.A., Straneo, F., Holte, J., Holliday, N.P., 2018. Seasonality of Freshwater in the East Greenland Current System From 2014 to 2016. *J. Geophys. Res. Oceans* 123, 8828–8848. <https://doi.org/10.1029/2018JC014511>
- Lee, Y.J., Maslowski, W., Cassano, J.J., Clement Kinney, J., Craig, A.P., Kamal, S., Osinski, R., Seefeldt, M.W., Stroeve, J., Wang, H., 2023. Causes and evolution of winter polynyas north of Greenland. *The Cryosphere* 17, 233–253. <https://doi.org/10.5194/tc-17-233-2023>
- 1020 Ludwig, V., Krumpen, T., 2026. Coverage varies, origin shifts: A review of 37 years of satellite-based sea-ice conditions around the HAUSGARTEN observatory. *Deep Sea Res. Part II Top. Stud. Oceanogr.* 227, 105638. <https://doi.org/10.1016/j.dsr2.2026.105638>
- Marnela, M., Rudels, B., Houssais, M.-N., Beszczynska-Möller, A., Eriksson, P.B., 2013. Recirculation in the Fram Strait and transports of water in and north of the Fram Strait derived from CTD data. *Ocean Sci.* 9, 499–519. <https://doi.org/10.5194/os-9-499-2013>
- 1025 McPherson, R.A., Von Appen, W.-J., De Steur, L., Kanzow, T., Beszczynska-Möller, A., Renner, A.H.H., 2026. Decades of change: Warming trends and hydrographic variability of Atlantic Water as observed in the west Spitsbergen current (1997–2024). *Deep Sea Res. Part II Top. Stud. Oceanogr.* 227, 105637. <https://doi.org/10.1016/j.dsr2.2026.105637>
- 1030 McPherson, R.A., Wekerle, C., Kanzow, T., 2023. Shifts of the Recirculation Pathways in Central Fram Strait Drive Atlantic Intermediate Water Variability on Northeast Greenland Shelf. *J. Geophys. Res. Oceans* 128, e2023JC019915. <https://doi.org/10.1029/2023JC019915>
- 1035 McPherson, R.A., Wekerle, C., Kanzow, T., Ionita, M., Heukamp, F.O., Zeising, O., Humbert, A., 2024. Atmospheric blocking slows ocean-driven melting of Greenland’s largest glacier tongue. *Science* 385, 1360–1366. <https://doi.org/10.1126/science.ado5008>
- Metfies, K., 2025. The Expedition PS143/2 of the Research Vessel POLARSTERN to the Arctic Ocean in 2024. Alfred-Wegener-Institut Helmholtz-Zentrum für Polar- und Meeresforschung. https://doi.org/10.57738/BZPM_0801_2025
- 1040 Olason, E., Notz, D., 2014. Drivers of variability in Arctic sea-ice drift speed. *J. Geophys. Res. Oceans* 119, 5755–5775. <https://doi.org/10.1002/2014JC009897>



- Polyakov, I.V., Ingvaldsen, R.B., Pnyushkov, A.V., Bhatt, U.S., Francis, J.A., Janout, M., Kwok, R., Skagseth, Ø., 2023. Fluctuating Atlantic inflows modulate Arctic atlantification. *Science* 381, 972–979. <https://doi.org/10.1126/science.adh5158>
- 1045 Polyakov, I.V., Pnyushkov, A.V., Alkire, M.B., Ashik, I.M., Baumann, T.M., Carmack, E.C., Goszczko, I., Guthrie, J., Ivanov, V.V., Kanzow, T., Krishfield, R., Kwok, R., Sundfjord, A., Morison, J., Rember, R., Yulin, A., 2017. Greater role for Atlantic inflows on sea-ice loss in the Eurasian Basin of the Arctic Ocean. *Science* 356, 285–291. <https://doi.org/10.1126/science.aai8204>
- Quadfasel, D., Gascard, J.-C., Koltermann, K.-P., 1987. Large-scale oceanography in Fram Strait during the 1984 Marginal Ice Zone Experiment. *J. Geophys. Res.* 92, 6719. <https://doi.org/10.1029/jc092ic07p06719>
- 1050 Rudels, B., 2002. The East Greenland Current and its contribution to the Denmark Strait overflow. *ICES J. Mar. Sci.* 59, 1133–1154. <https://doi.org/10.1006/jmsc.2002.1284>
- Rudels, B., Quadfasel, D., 1991. Convection and deep water formation in the Arctic Ocean-Greenland Sea System. *J. Mar. Syst.* 2, 435–450. [https://doi.org/10.1016/0924-7963\(91\)90045-V](https://doi.org/10.1016/0924-7963(91)90045-V)
- 1055 Schaffer, J., von Appen, W.-J., Dodd, P.A., Hofstede, C., Mayer, C., de Steur, L., Kanzow, T., 2017. Warm water pathways toward Nioghalvfjærdsfjorden Glacier, Northeast Greenland. *J. Geophys. Res. Oceans* 122, 4004–4020. <https://doi.org/10.1002/2016JC012462>
- Skagseth, Ø., Furevik, T., Ingvaldsen, R., Loeng, H., Mork, K.A., Orvik, K.A., Ozhigin, V., 2008. Volume and Heat Transports to the Arctic Ocean Via the Norwegian and Barents Seas, in: Dickson, R.R., Meincke, J., Rhines, P. (Eds.), *Arctic–Subarctic Ocean Fluxes*. Springer Netherlands, Dordrecht, pp. 45–64. https://doi.org/10.1007/978-1-4020-6774-7_3
- 1060 Smedsrud, L.H., Halvorsen, M.H., Stroeve, J.C., Zhang, R., Kloster, K., 2017. Fram Strait sea ice export variability and September Arctic sea ice extent over the last 80 years. *The Cryosphere* 11, 65–79. <https://doi.org/10.5194/tc-11-65-2017>
- 1065 Spreen, G., De Steur, L., Divine, D., Gerland, S., Hansen, E., Kwok, R., 2020. Arctic Sea Ice Volume Export Through Fram Strait From 1992 to 2014. *J. Geophys. Res. Oceans* 125. <https://doi.org/10.1029/2019jc016039>
- Spreen, G., Kaleschke, L., Heygster, G., 2008. Sea ice remote sensing using AMSR-E 89-GHz channels. *J. Geophys. Res. Oceans* 113, 2005JC003384. <https://doi.org/10.1029/2005JC003384>
- 1070 Straneo, F., Sutherland, D.A., Holland, D., Gladish, C., Hamilton, G.S., Johnson, H.L., Rignot, E., Xu, Y., Koppes, M., 2012. Characteristics of ocean waters reaching Greenland’s glaciers. *Ann. Glaciol.* 53, 202–210. <https://doi.org/10.3189/2012AoG60A059>
- Sumata, H., de Steur, L., Divine, D.V., Granskog, Mats.A., Gerland, S., 2023. Regime shift in Arctic Ocean sea ice thickness. *Nature* 615, 443–449. <https://doi.org/10.1038/s41586-022-05686-x>
- 1075 Sumata, H., De Steur, L., Gerland, S., Divine, D.V., Pavlova, O., 2022. Unprecedented decline of Arctic sea ice outflow in 2018. *Nat. Commun.* 13, 1747. <https://doi.org/10.1038/s41467-022-29470-7>
- Sutherland, D.A., Pickart, R.S., 2008. The East Greenland Coastal Current: Structure, variability, and forcing. *Prog. Oceanogr.* 78, 58–77. <https://doi.org/10.1016/j.pocean.2007.09.006>
- Voet, G., Quadfasel, D., Mork, K.A., Søiland, H., 2010. The mid-depth circulation of the Nordic Seas derived from profiling float observations. *Tellus A* 62, 516–529. <https://doi.org/10.1111/j.1600-0870.2010.00444.x>
- 1080



- von Appen, W.-J., Schauer, U., Hattermann, T., Beszczynska-Möller, A., 2016. Seasonal Cycle of Mesoscale Instability of the West Spitsbergen Current. *J. Phys. Oceanogr.* 46, 1231–1254. <https://doi.org/10.1175/JPO-D-15-0184.1>
- 1085 Wekerle, C., Hattermann, T., Wang, Q., Crews, L., Von Appen, W.J., Danilov, S., 2020. Properties and dynamics of mesoscale eddies in Fram Strait from a comparison between two high-resolution ocean-sea ice models. *Ocean Sci.* 16, 1225–1246. <https://doi.org/10.5194/os-16-1225-2020>
- 1090 Wekerle, C., McPherson, R., Von Appen, W.-J., Wang, Q., Timmermann, R., Scholz, P., Danilov, S., Shu, Q., Kanzow, T., 2024. Atlantic Water warming increases melt below Northeast Greenland's last floating ice tongue. *Nat. Commun.* 15, 1336. <https://doi.org/10.1038/s41467-024-45650-z>
- Woodgate, R.A., Fahrbach, E., Rohardt, G., 1999. Structure and transports of the East Greenland Current at 75°N from moored current meters. *J. Geophys. Res. Oceans* 104, 18059–18072. <https://doi.org/10.1029/1999JC900146>